28. Nolan MF, Dudman JT, Dodson PD, Santoro B: **HCN1 channels control resting and active integrative properties of stellate cells from layer II of the entorhinal cortex.** *J Neurosci* 2007, **27**:12440–12451.
29. Setou M, Nakagawa T, Seog DH, Hirokawa N: **Kinesin superfamily motor protein KIF17 and mLin-10 in NMDA receptor-containing vesicle transport.** *Science* 2000, **288**:1796–1802.
30. Saito Y, Akiyama M, Araki Y, Sumioka A, Shiono M, *et al*: **Intracellular Trafficking of the Amyloid β-Protein Precursor (APP) Regulated by Novel Function of X11-Like.** *PLoS One* 2011, **6**:e22108.
31. Braak H, Braak E: **Neuropathological stageing of Alzheimer-related changes.** *Acta Neuropathol* 1991, **82**:239–259.
32. Nakamura S, Nakayama H, Goto N, Ono F, Sakakibara I, Yoshikawa Y: **Histopathological studies of senile plaques and cerebral amyloidosis in cynomolgus monkeys.** *J Med Primatol* 1998, **27**:244–252.
33. Oikawa N, Kimura N, Yanagisawa K: **Alzheimer-type tau pathology in advanced aged nonhuman primate brains harboring substantial amyloid deposition.** *Brain Res* 2010, **1315**:137–149.
34. Podlisny MB, Tolan DR, Selkoe DJ: **Homology of the amyloid β protein precursor in monkey and human supports a primate model for β amyloidosis in Alzheimer's disease.** *Am J Pathol* 1991, **138**:1423–1435.
35. Rogelj B, Mitchell JC, Miller CCJ, McLoughlin DM: **The X11/Mint family of adaptor proteins.** *Brain Res Rev* 2006, **52**:305–315.
36. Shah MM, Anderson AE, Leung V, Lin X, Johnston D: **Seizure-induced plasticity of h channels in entorhinal cortical layer III pyramidal neurons.** *Neuron* 2004, **44**:495–508.
37. Powell KL, Ng C, O'Brien TJ, Xu SH, Williams DA, *et al*: **Decreases in HCN mRNA expression in the hippocampus after kindling and status epilepticus in adult rats.** *Epilepsia* 2008, **49**:1686–1695.
38. Bender RA, Soleymani SV, Brewster AL, Nguyen ST, Beck H, *et al*: **Enhanced expression of a specific hyperpolarization-activated cyclic nucleotide-gated cation channel (HCN) in surviving dentate gyrus granule cells of human and experimental epileptic hippocampus.** *J Neurosci* 2003, **23**:6826–6836.
39. Brewster A, Bender RA, Chen Y, Dube C, Eghbal Ahmadi M, Baram TZ: **Developmental febrile seizures modulate hippocampal gene expression of hyperpolarization-activated channels in an isoform- and cell-specific manner.** *J Neurosci* 2002, **22**:4591–4599.
40. Dugladze T, Vida I, Tort AB, Gross A, Otahal J, *et al*: **Impaired hippocampal rhythmogenesis in a mouse model of mesial temporal lobe epilepsy.** *Proc Natl Acad Sci USA* 2007, **104**:17530–17535.
41. Jung S, Jones TD, Lugo JN Jr, Sheerin AH, Miller JW, *et al*: **Progressive dendritic HCN channelopathy during epileptogenesis in the rat pilocarpine model of epilepsy.** *J Neurosci* 2007, **27**:13012–13021.
42. Shin M, Brager D, Jaramillo TC, Johnston D, Chetkovich DM: **Mislocalization of h channel subunits underlies h channelopathy in temporal lobe epilepsy.** *Neurobiol Dis* 2008, **32**:26–36.
43. Marcelin B, Chauviere L, Becker A, Migliore M, Esclapez M, Bernard C: **h channel-dependent deficit of theta oscillation resonance and phase shift in temporal lobe epilepsy.** *Neurobiol Dis* 2009, **33**:436–447.
44. Nie Z, Hirsch DS, Randazzo PA: **Arf and its many interactors.** *Curr Opin Cell Biol* 2003, **15**:396–404.
45. Teber I, Nagano F, Kremerskothen J, Bilbilis K, Goud B, Barnekow A: **Rab6 interacts with the mint3 adaptor protein.** *Biol Chem* 2005, **386**: 671–677.
46. Araki Y, Tomita S, Yamaguchi H, Miyagi N, Sumioka A, *et al*: **Novel cadherin-related membrane proteins, Alcadeins, enhance the X11-like protein-mediated stabilization of amyloid beta-protein precursor metabolism.** *J Biol Chem* 2003, **278**:49448–49458.
47. Araki Y, Kawano T, Taru H, Saito Y, Wada S, *et al*: **The novel cargo Alcadein induces vesicle association of kinesin-1 motor components and activates axonal transport.** *EMBO J* 2007, **26**:1475–1486.
48. Kakuda N, Shoji M, Arai H, Furukawa K, Ikeuchi T, *et al*: **Altered γ-secretase activity in mild cognitive impairment and Alzheimer's disease.** *EMBO Mol Med* 2012, **4**:344–352.
49. Ishii TM, Takano M, Ohmori H: **Determinants of activation kinetics in mammalian hyperpolarization-activated cation channels.** *J Physiol* 2001, **537**:99–100.
50. Zhu G, Okada M, Yoshida S, Ueno S, Mori F, *et al*: **Rats harboring S284L Chrna4 mutation show attenuation of synaptic and extrasynaptic GABAergic transmission and exhibit the nocturnal frontal lobe epilepsy phenotype.** *J Neurosci* 2008, **28**:12465–12376.
51. Dickson CT, Magistretti J, Shalinsky MH, Fransen E, Hasselmo ME, Alonso A: **Properties and role of I(h) in the pacing of subthreshold oscillations in entorhinal cortex layer II neurons.** *J Neurophysiol* 2000, **83**:2562–2579.

doi:10.1186/1750-1326-7-50
Cite this article as: Saito *et al.*: Hyperpolarization-activated cyclic nucleotide gated channels: a potential molecular link between epileptic seizures and Aβ generation in Alzheimer's disease. *Molecular Neurodegeneration* 2012 7:50.

Amyotrophic Lateral Sclerosis, 2012; 13: 562–566

informa
healthcare

ORIGINAL ARTICLE

Mutational analysis of familial and sporadic amyotrophic lateral sclerosis with *OPTN* mutations in Japanese population

HIROYA NARUSE[1], YUJI TAKAHASHI[1], TAMEKO KIHIRA[2], SOHEI YOSHIDA[2], YASUMASA KOKUBO[3], SHIGEKI KUZUHARA[4], HIROYUKI ISHIURA[1], MASAHARU AMAGASA[5], SHIGEO MURAYAMA[6], SHOJI TSUJI[1] & JUN GOTO[1]

[1]*Department of Neurology, Graduate School of Medicine, The University of Tokyo, Tokyo,* [2]*Kansai University of Health Sciences, Kumatori, Osaka,* [3]*Department of Neurology, Mie University School of Medicine, Tsu, Mie,* [4]*Department of Medical Welfare, Suzuka University of Medical Science, Suzuka, Mie,* [5]*Department of Neurology and Neurosurgery, Yamagata Tokushukai Hospital, Yamagata, and* [6]*Geriatric Neuroscience (Neuropathology), Tokyo Metropolitan Institute of Gerontology, Tokyo, Japan*

Abstract

Our objective was to elucidate the genetic epidemiology of familial amyotrophic lateral sclerosis (FALS) and sporadic ALS (SALS) with *OPTN* mutations in the Japanese population. Mutational analysis of *OPTN* was conducted in 18 FALS pedigrees in whom mutations in other causative genes have been excluded and in 218 SALS patients by direct nucleotide sequence analysis. Novel non-synonymous variants identified in ALS patients were further screened in 271 controls. Results showed that although no mutations were identified in the FALS pedigrees, a novel heterozygous non-synonymous variant c.481G>A (p.V161M) was identified in one SALS patient, who originated from the southernmost part of the Kii Peninsula. The mutation was not present in 271 controls. As the clinical feature, the patient carrying V161M showed predominantly upper motor neuron signs with slow progression. This study suggests that mutations in *OPTN* are not the main cause of ALS in the Japanese population.

Key words: *Motor neuron disease, amyotrophic lateral sclerosis, OPTN mutation, genetic analysis, V161M*

Introduction

Molecular genetic research on amyotrophic lateral sclerosis (ALS) has revealed a number of causative genes for familial ALS (FALS), which include *SOD1* (1), *ALS2* (2,3), *DCTN1* (4), *VAPB* (5), *CHMP2B* (6), *ANG* (7), *TARDBP* (8), and *FUS* (9,10). These genes collectively account for approximately 30% of FALS pedigrees (11). Mutations in these genes have also been identified in some sporadic ALS (SALS) patients, suggesting mutations with reduced penetrance or *de novo* mutations (12,13). Recently, hexanucleotide repeat expansion within the *C9ORF72* gene has been reported to be associated with a large proportion of cases of ALS and frontotemporal dementia (FTD) with wider European ancestry (14–16). Mutations in *UBQLN2* were also identified to cause dominant X-linked juvenile and adult-onset ALS and ALS/dementia (17). *OPTN*, which was previously identified as the causative gene for rare autosomal dominant familial primary open-angle glaucoma (POAG), has been reported as the causative gene for autosomal dominant and autosomal recessive FALS (18). Subsequent genetic epidemiological studies on *OPTN* mutations in different cohorts have revealed that frequencies of mutations in patients with FALS and SALS vary among cohorts, from 0% to 4.35% (pedigree frequency) in those with FALS, and from 0% to 3.54% (case frequency) in those with SALS (18–23). Further analyses on larger cohorts of various ethnic backgrounds will be necessary to establish the genetic epidemiology and clinical characteristics of ALS and the genotype-phenotype correlations of ALS with *OPTN* mutations. We conducted further mutational analysis of *OPTN* in our cohorts to establish the molecular epidemiology of ALS in patients with mutations in *OPTN*.

Correspondence: J. Goto, Department of Neurology, Graduate School of Medicine, The University of Tokyo, 7-3-1 Hongo, Bunkyo-ku, Tokyo 113-8655, Japan. Fax: 81 3 5800 6844. E-mail: gotoj-tky@umin.ac.jp

(Received 15 December 2011; accepted 2 April 2012)

ISSN 1748-2968 print/ISSN 1471-180X online © 2012 Informa Healthcare
DOI: 10.3109/17482968.2012.684213

Materials and methods

Thirty-five FALS pedigrees, 218 SALS patients, and 271 controls, all of whom were from the Japanese population, were enrolled in this study. Of the 35 FALS pedigrees, 17 harbored causative mutations in other causative genes for FALS with the autosomal dominant mode of inheritance. The remaining 18 pedigrees consisted of 13 with the autosomal dominant mode of inheritance, two pedigrees with affected sibs with consanguinity, and three pedigrees with affected sibs without consanguinity. The 218 SALS patients, most of whom visited the University of Tokyo Hospital, included 33 from Yamagata Prefecture, on the northern part of Honshu island, and 15 from the Kii Peninsula, on the southern part of Honshu island. The mean age at onset of the SALS cohort was 58.9 years, and the male: female ratio was 3: 2. All of the genomic DNA samples were obtained from the participants of this study with their written informed consent, and this research was approved by the Institutional Review Board of the University of Tokyo.

Mutational analysis

Mutations in causative genes for FALS were analyzed employing a DNA microarray-based resequencing system as described elsewhere (24) or a direct nucleotide sequencing method conducted using a BigDye Terminator ver. 3.1 cycle sequencing kit on a 3100 ABI Prism Genetic Analyzer (Applied Biosystems). All the coding exons of *OPTN* (exons 4–16) were amplified by genomic PCR using specific primers for each exon recently reported (18) and further subjected to direct nucleotide sequence analysis.

Mutations in other causative genes for FALS, including *SOD1, ALS2, DCTN1, VAPB, CHMP2B, ANG*, and *TARDBP*, were firstly excluded employing a DNA microarray-based resequencing system. Secondary, mutational analysis of *FUS* employing a direct nucleotide sequencing method was performed. The remaining samples were subjected to mutational analysis of *OPTN* by direct nucleotide sequence analysis.

The variants identified by the mutational analysis were evaluated using databases of dbSNP (http://www.ncbi.nlm.nih.gov/SNP/index.html), 1000 Genomes Project (http://www.1000genomes.org/), and Exome Sequencing Project (https://esp.gs.washington.edu/). When novel non-synonymous variants not registered in these databases were identified, they were further screened in 271 controls by direct nucleotide sequence analysis. The effect of amino acid changes caused by identified novel variants was predicted using the PolyPhen-2 website (http://genetics.bwh.harvard.edu/pph2/).

Results

Of the 35 FALS pedigrees enrolled in this study, 17 harbored causative mutations in other causative genes for FALS including 14 *SOD1*, two *FUS*, and one *TARDBP*. The remaining 18 pedigrees were subjected to mutational analysis of *OPTN*. Five variants including four known SNPs and a novel synonymous variant in exon 16 were identified (Table I). We did not observe any causative mutations in *OPTN* in the FALS pedigrees in our cohort.

In the 218 SALS patients, seven variants including four known SNPs, two novel synonymous variants in exons 4 and 7, and one novel non-synonymous variant in exon 6 not registered in dbSNPs, 1000 Genomes Project, or Exome Sequencing Project were identified (Table II). Known causative mutations for ALS were not identified in the SALS patients. The novel heterozygous non-synonymous variant of c.481G >A in exon 6 substituting methionine for valine at amino acid position 161 (p.V161M) was identified in a SALS patient (Figure 1A, B). This novel variant of V161M was not present in 271 controls (542 chromosomes). Although the amino acid valine at position 161 was not necessarily highly conserved among species (Figure 1C), the PolyPhen-2 prediction was possibly damaging with a score of 0.913.

Interestingly, the patient with V161M mutation originated from the southernmost part of the Kii Peninsula, where the prevalence of ALS is high and patients with the ALS-parkinsonism-dementia

Table I. Summary of *OPTN* variants identified in 18 FALS patients.

Exon	SNP ID*	Base changes	Annotation	Amino acid changes	Number of pedigrees (Allele frequency)		Allele frequency (1000 Genomes)**
4	rs2234968	c.102G>A	Synonymous		3 homozygotes, 1 heterozygote#	(0.389)	0.182
5	rs11258194	c.293T>A	Non-synonymous	p.Met98Lys	1 heterozygote	(0.028)	0.110
10	rs523747	c.964A>G	Non-synonymous	p.Lys322Glu	18 homozygotes	(1.000)	1.000
16	rs75654767	c.1634G>A	Non-synonymous	p.Arg545Gln	2 heterozygotes#	(0.056)	0.028
16	Novel	c.1713C>T	Synonymous		1 heterozygote	(0.028)	0.000

*SNP ID is the single-nucleotide polymorphism identification obtained from dbSNP database.
**The allele frequencies in East Asian populations were obtained from 1000 Genomes Project (http://www.1000genomes.org/).
#One patient carried both the heterozygous c.102G>A variant and the heterozygous c.1634G>A variant.

Table II. Summary of *OPTN* variants identified in 218 SALS patients.

Exon	SNP ID*	Base changes	Annotation	Amino acid changes	Number of cases (Allele frequency)		Allele frequency (1000 Genomes)**
4	rs2234968	c.102G>A	Synonymous		3 homozygotes, 59 heterozygotes	(0.149)	0.182
4	Novel	c.147C>T	Synonymous		1 homozygote	(0.004)	0.000
5	rs11258194	c.293T>A	Non-synonymous	p.Met98Lys	17 heterozygotes	(0.039)	0.110
6	Novel	c.481G>A	Non-synonymous	p.Val161Met	1 heterozygote	(0.002)	0.000
7	Novel	c.630A>T	Synonymous		1 heterozygote	(0.002)	0.000
10	rs523747	c.964A>G	Non-synonymous	p.Lys322Glu	218 homozygotes	(1.000)	1.000
16	rs75654767	c.1634G>A	Non-synonymous	p.Arg545Gln	13 heterozygotes	(0.030)	0.028

*SNP ID is the single-nucleotide polymorphism identification obtained from dbSNP database.
**The allele frequencies in East Asian populations were obtained from 1000 Genomes Project (http://www.1000genomes.org/).

complex are clustered. We further conducted the mutational analysis of *OPTN* recruiting four additional patients with SALS in the same district. These patients, however, harbored neither the V161M mutation nor any other mutations in *OPTN*.

The clinical features of the patient with the V161M mutation are briefly presented as follows. The patient was a 35-year-old male at the time of diagnosis of ALS, who developed upper extremity weakness for one year. Weakness and atrophy predominantly in upper extremities gradually worsened. Neurological examination at the age of 39 years revealed tongue atrophy and fasciculation, attenuated tendon reflexes and muscle wasting in the upper extremities, and enhanced tendon reflexes in the lower extremities with bilateral extensor plantar reflexes. He became mechanical-ventilator-dependent at the age of 50 years. There was no evidence of parkinsonism or cognitive impairment at the age of 50 years. His medical history included unexplained vision loss of his right eye in his childhood. His father, who also originated from the southernmost part of the Kii Peninsula, was alive and did not show any symptoms indicative of motor neuron disease when the index patient was 35 years old. His mother, who originated from southeastern part of the Kii Peninsula, died of liver cirrhosis, but her age at death was not indicated.

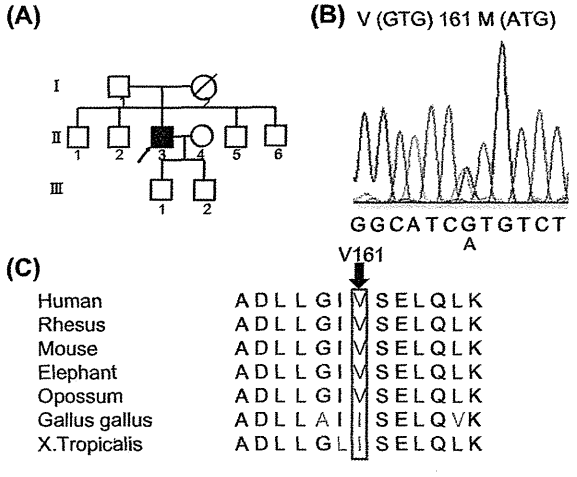

Figure 1. (A) Pedigree chart of patient with V161M variant in *OPTN*. Affected individuals are indicated by filled symbols. The proband is indicated by an arrow. Unaffected individuals are indicated by open symbols. Slashed symbols indicate deceased subjects. Ages at death are shown when information is available. Squares denote male family members and circles denote female family members. (B) Electropherogram of heterozygous *OPTN* c.481G>A (p.Val161Met) point mutation. (C) Conservation of *OPTN* amino acid sequences among different animal species. The valine residue at codon 161 is not necessarily highly conserved among different species (shown in red). Non-conserved amino acids are shown in green.

Discussion

In this study, we conducted a comprehensive mutational analysis of *OPTN* in a large cohort of Japanese FALS and SALS patients. Among our 35 FALS pedigrees, 17 families had mutations in other causative genes previously reported, as described in Results, and we did not find any causative mutations in *OPTN* in the remaining 18 pedigrees. On the other hand, among the 218 patients with SALS, we identified a patient carrying a novel non-synonymous mutation of *OPTN*.

Previous genetic studies on *OPTN* mutations in different cohorts have demonstrated that the frequencies of *OPTN* mutations are from 0% to 4.35% (pedigree frequency) in FALS (18–23) (Table IIIA). *OPTN* was initially identified as a causative gene for FALS in a consanguineous pedigree through homozygosity mapping followed by sequencing of candidate genes in the homozygous region. In our cohort, autosomal recessive inheritance was suggested in only five of the 35 FALS families, which may account for the fact that we did not identify any causative mutations in *OPTN* in the FALS families. Since the number of families enrolled in this study is limited, further extensive mutational analysis of larger cohorts of FALS will be necessary to establish the genetic epidemiology of FALS patients with *OPTN* mutations.

In our SALS cohort, a novel heterozygous non-synonymous variant, V161M, was identified in a patient. Previous genetic studies on *OPTN* mutations in different cohorts have shown a number of heterozygous missense mutations in SALS patients (20,21) and that the frequencies of *OPTN* mutations are from 0% to 3.54% (case frequency) in SALS (18–23) (Table IIIB). When we assess the implication of the

Table IIIA. Summary of *OPTN* variants identified in FALS patients in previous and present studies.

Studies	Ethnicity	Variant	Number of pedigrees	Status
Maruyama H, et al.[18]	Japanese	exon 5 deletion	4	1 homozygote
		p.Q398X		1 homozygote
		p.E478G		2 heterozygotes
Belzil VV, et al.[19]	European	c.1242+1G>A_insA	2	1 heterozygote
		p.A481V		1 heterozygote
Del Bo R, et al.[20]	Italian	p.G23X	2	1 heterozygote
		p.K557T		1 heterozygote
Iida A, et al.[21]	Japanese	p.E478G	1	1 homozygote
Millecamps S, et al.[22]	Caucasian	p.R96L	1	1 heterozygote
Sugihara K, et al.[23]	Caucasian	None	0	
Present study	Japanese	None	0	

mutation identified in an isolated case without any family history, we need to carefully consider various possibilities including the possibilities of causative mutation with reduced penetrance and *de novo* mutation. Another possibility is that the variant might not necessarily be associated with a risk of ALS.

Hexanucleotide repeat expansion within the *C9ORF72* gene has very recently been reported to be frequent as a cause of ALS with wider European ancestry. Our recent study on the same cohort indicated that the frequency of the patients with the hexanucleotide repeat expansions is very low (16), suggesting that the result of our molecular epidemiology study of *OPTN* was not substantially affected by that of *C9ORF72* in our Japanese cohort.

Previous studies showed that the clinical phenotypes of patients with *OPTN* mutations are heterogeneous for both age of onset and disease duration, but are characterized by a relatively slow progression, lower-limb onset, and frequent upper motor neuron signs. The relatively slow progression after the onset and the presence of upper motor neuron signs observed in the patient with the V161M variant are consistent with the previous reports (18–23). However, this patient differed from those in previous reports to the extent that the onset site is the upper extremities. Further accumulation of clinical information is essential to delineate the phenotypic spectrum and to illustrate the genotype-phenotype correlations of ALS with *OPTN* mutations.

Of note, the patient originated from the southernmost part of the Kii Penisula including the Koza River, where the prevalence of ALS has been described to be higher than in other areas of Japan (25). Neither the causes of the high prevalence nor the genetic risk factors common to ALS patients in the region have been elucidated. Mutational analysis of four additional ALS patients residing in the same district (Koza River and its vicinity), however, revealed neither the V161M mutation nor other mutations. V161M does not appear to be very common among the patients with ALS in this district.

Acknowledgements

We thank all patients and their family members for participating in this study. This work was supported in part by KAKENHI (Grant-in-Aid for Scientific Research on Innovative Areas) and Global COE Program from the Ministry of Education, Culture, Sports, Science and Technology of Japan, and a Grant-in-Aid for Research on Intractable Diseases and Comprehensive Research on Disability Health and Welfare from the Ministry of Health, Welfare and Labor, Japan.

Declaration of interest: The authors report no conflicts of interest. The authors alone are responsible for the content and writing of the paper.

Table IIIB. Summary of *OPTN* variants identified in SALS patients in previous and present studies.

Studies	Ethnicity	Variant	Number of cases	Status
Maruyama H, et al.[18]	Japanese	p.Q398X	1	1 homozygote
Belzil VV, et al.[19]	European	None	0	
Del Bo R, et al.[20]	Italian	c.552+1delG	4	1 heterozygote
		p.T282P		1 heterozygote
		p.Q314L		1 heterozygote
		c.1401+4A>G		1 heterozygote
Iida A, et al.[21]	Japanese	p.A93P	2	1 heterozygote
		p.E478G		1 heterozygote
Sugihara K, et al.[23]	Caucasian	None	0	
Present study	Japanese	p.V161M	1	1 heterozygote

References

1. Rosen DR, Siddique T, Patterson D, Figlewicz DA, Sapp P, Hentati A, et al. Mutations in Cu/Zn superoxide dismutase gene are associated with familial amyotrophic lateral sclerosis. Nature. 1993;362:59–62.
2. Hadano S, Hand CK, Osuga H, Yanagisawa Y, Otomo A, Devon RS, et al. A gene encoding a putative GTPase regulator is mutated in familial amyotrophic lateral sclerosis 2. Nat Genet. 2001;29:166–73.
3. Yang Y, Hentati A, Deng HX, Dabbagh O, Sasaki T, Hirano M, et al. The gene encoding alsin, a protein with three guanine-nucleotide exchange factor domains, is mutated in a form of recessive amyotrophic lateral sclerosis. Nat Genet. 2001;29:160–5.
4. Puls I, Jonnakuty C, LaMonte BH, Holzbaur EL, Tokito M, Mann E, et al. Mutant dynactin in motor neuron disease. Nat Genet. 2003;33:455–6.
5. Nishimura AL, Mitne-Neto M, Silva HC, Richieri-Costa A, Middleton S, Cascio D, et al. A mutation in the vesicle-trafficking protein VAPB causes late-onset spinal muscular atrophy and amyotrophic lateral sclerosis. Am J Hum Genet. 2004;75:822–31.
6. Parkinson N, Ince PG, Smith MO, Highley R, Skibinski G, Andersen PM, et al. ALS phenotypes with mutations in CHMP2B (charged multivesicular body protein 2B). Neurology. 2006;67:1074–7.
7. Greenway MJ, Andersen PM, Russ C, Ennis S, Cashman S, Donaghy C, et al. ANG mutations segregate with familial and sporadic amyotrophic lateral sclerosis. Nat Genet. 2006;38:411–3.
8. Kabashi E, Valdmanis PN, Dion P, Spiegelman D, McConkey BJ, Vande Velde C, et al. TARDBP mutations in individuals with sporadic and familial amyotrophic lateral sclerosis. Nat Genet. 2008;40:572–4.
9. Kwiatkowski TJ Jr, Bosco DA, Leclerc AL, Tamrazian E, Vanderburg CR, Russ C, et al. Mutations in the FUS/TLS gene on chromosome 16 cause familial amyotrophic lateral sclerosis. Science. 2009;323:1205–8.
10. Vance C, Rogelj B, Hortobágyi T, de Vos KJ, Nishimura AL, Sreedharan J, et al. Mutations in FUS, an RNA processing protein, cause familial amyotrophic lateral sclerosis type 6. Science. 2009;323:1208–11.
11. Dion PA, Daoud H, Rouleau GA. Genetics of motor neuron disorders: new insights into pathogenic mechanisms. Nat Rev Genet. 2009;10:769–82.
12. Alexander MD, Traynor BJ, Miller N, Corr B, Frost E, McQuaid S, et al. 'True' sporadic ALS associated with a novel SOD1 mutation. Ann Neurol. 2002;52:680–3.
13. Chiò A, Calvo A, Moglia C, Ossola I, Brunetti M, Sbaiz L, et al. A de novo missense mutation of the FUS gene in a 'true' sporadic ALS case. Neurobiol Aging. 2011;32: 553.e23–6.
14. DeJesus-Hernandez M, Mackenzie IR, Boeve BF, Boxer AL, Baker M, Rutherford NJ, et al. Expanded GGGGCC hexanucleotide repeat in non-coding region of C9ORF72 causes chromosome 9p-linked FTD and ALS. Neuron. 2011;72:245–56.
15. Renton AE, Majounie E, Waite A, Simon-Sanchez J, Rollinson S, Gibbs JR, et al. A hexanucleotide repeat expansion in C9ORF72 is the cause of chromosome 9p21-linked ALS-FTD. Neuron. 2011;72:257–68.
16. Majounie E, Renton AE, Mok K, Dopper EG, Waite A, Rollinson S, et al. Frequency of the C9orf72 hexanucleotide repeat expansion in patients with amyotrophic lateral sclerosis and frontotemporal dementia: a cross-sectional study. Lancet Neurol. 2012;11:323–30.
17. Deng HX, Chen W, Hong ST, Boycott KM, Gorrie GH, Siddique N, et al. Mutations in UBQLN2 cause dominant X-linked juvenile and adult-onset ALS and ALS/dementia. Nature. 2011;477:211–5.
18. Maruyama H, Morino H, Ito H, Izumi Y, Kato H, Watanabe Y, et al. Mutations of optineurin in amyotrophic lateral sclerosis. Nature. 2010;465:223–6.
19. Belzil VV, Daoud H, Desjarlais A, Bouchard JP, Dupré N, Camu W, et al. Analysis of OPTN as a causative gene for amyotrophic lateral sclerosis. Neurobiol Aging. 2011;32:555.e13–4.
20. Del Bo R, Tiloca C, Pensato V, Corrado L, Ratti A, Ticozzi N, et al. Novel optineurin mutations in patients with familial and sporadic amyotrophic lateral sclerosis. J Neurol Neurosurg Psychiatry. 2011;82:1239–43.
21. Iida A, Hosono N, Sano M, Kamei T, Oshima S, Tokuda T, et al. Optineurin mutations in Japanese amyotrophic lateral sclerosis. J Neurol Neurosurg Psychiatry. 2012;83:233–5.
22. Millecamps S, Boillée S, Chabrol E, Camu W, Cazeneuve C, Salachas F, et al. Screening of OPTN in French familial amyotrophic lateral sclerosis. Neurobiol Aging. 2011;32: 557.e11–3.
23. Sugihara K, Maruyama H, Kamada M, Morino H, Kawakami H. Screening for OPTN mutations in amyotrophic lateral sclerosis in a mainly Caucasian population. Neurobiol Aging. 2011;32:1923.e9–10.
24. Takahashi Y, Seki N, Ishiura H, Mitsui J, Matsukawa T, Kishino A, et al. Development of a high-throughput microarray-based resequencing system for neurological disorders and its application to molecular genetics of amyotrophic lateral sclerosis. Arch Neurol. 2008;65:1326–32.
25. Yoshida S, Uebayashi Y, Kihira T, Kohmoto J, Wakayama I, Taguchi S, et al. Epidemiology of motor neuron disease in the Kii Peninsula of Japan, 1989–1993: active or disappearing focus? J Neurol Sci. 1998;155:146–55.

J Neuropathol Exp Neurol

Vol. 71, No. 7
July 2012
pp. 625–630

ORIGINAL ARTICLE

α-Synuclein Pathology in the Amyotrophic Lateral Sclerosis/ Parkinsonism Dementia Complex in the Kii Peninsula, Japan

Yasumasa Kokubo, MD, PhD, Akira Taniguchi, MD, Masato Hasegawa, PhD, Yuma Hayakawa, Satoru Morimoto, MD, Misao Yoneda, PhD, Yoshihumi Hirokawa, MD, PhD, Taizo Shiraishi, MD, PhD, Yuko Saito, MD, PhD, Shigeo Murayama, MD, PhD, and Shigeki Kuzuhara, MD, PhD

Abstract

α-Synuclein pathology was examined in the brains and spinal cords of 10 patients with amyotrophic lateral sclerosis (ALS)/parkinsonism-dementia complex (PDC) in the Kii Peninsula, Japan. Various types of phosphorylated α-synuclein–positive structures including neuronal cytoplasmic inclusions, dystrophic neurites, and glial cytoplasmic inclusions were found in all ALS/PDC cases. There were phosphorylated α-synuclein–positive neurons in 8 cases (80%), and the amygdala was most severely affected. Phosphorylated α-synuclein was distributed mainly in the limbic system and brainstem; tau pathology was more prevalent than α-synuclein pathology in most affected areas. In the substantia nigra, periaqueductal gray, locus coeruleus, raphe nuclei, dorsal nucleus of the vagus nerve, hypoglossal nucleus or ventral horn, and intermediolateral nucleus of the spinal cord, α-synuclein pathology was more predominant than tau pathology in only 1 or 2 patients. Phosphorylated α-synuclein– positive structures were not found in the molecular layer of the cerebellum. Phosphorylated α-synuclein frequently colocalized with tau in neuron cell bodies, neurites, and glia. Immunoblots of sarkosyl-insoluble fractions extracted from the brain of 1 patient showed a triplet of α-synuclein–immunoreactive bands that were ubiquitinated. These results suggest that interaction between tau and α-synuclein be involved in the pathogenesis of Kii ALS/PDC.

Key Words: α-Synuclein, Amyotrophic lateral sclerosis, Guam, Kii Peninsula, Parkinsonism-dementia complex, Tau.

From the Departments of Neurology (YK, AT), and Pathology (MY, YHi, TS), Mie University Graduate School of Medicine, Mie; Department of Molecular Neurobiology (MH), Tokyo Metropolitan Institute of Medical Science; Department of Neuropathology (SMo, SMu), Metropolitan Institute of Gerontology; Department of Neuropathology (YS), National Center of Neurology and Psychiatry, Tokyo; and Department of Medical Welfare (SK), Suzuka University of Medical Science, Mie, Japan.

Send correspondence and reprint requests to: Yasumasa Kokubo, MD, PhD, Department of Neurology, Mie University Graduate School of Medicine, 2-174 Edobashi, Tsu, Mie 514-8507, Japan; E-mail: kokubo-y@clin.medic.mie-u.ac.jp

Yuma Hayakawa is a medical student at the Mie University School of Medicine, Mie, Japan.

This study was supported in part by a Grant-in-Aid of the Nagao Memorial Fund, the Mie Medical Fund, by a Grant-in-Aid of the Research Committee of CNS Degenerative Diseases and Muro Disease (Kii ALS/PDC), the Ministry of Health, Labor and Welfare, Japan (Grant 21210301 to Y.K.), and by a Grant-in-Aid for Scientific Research from the Ministry of Education, Science, Sports and Culture, Japan.

INTRODUCTION

Amyotrophic lateral sclerosis/parkinsonism-dementia complex (ALS/PDC) is a neurodegenerative disease endemic to Guam and the Kii Peninsula of Japan (1–3). The clinical picture of ALS/PDC is a unique combination of parkinsonism, dementia, and symptoms of upper and lower motor neuronal dysfunction. Neuropathologic findings of ALS/PDC include numerous neurofibrillary tangles (NFTs) associated with nerve cell loss in the cerebral cortex and brainstem in addition to ALS pathology. Our investigation of the topographical distribution of NFTs suggested that ALS and PDC in the Kii Peninsula comprise part of a spectrum of tauopathies (4).

α-Synuclein is a presynaptic protein. Phosphorylated α-synuclein is the main component of Lewy bodies (LBs) that are characteristic of Parkinson disease and dementia with LBs (DLB), and of the glial cytoplasmic inclusions found in multiple system atrophy (5, 6). In Guamanian patients with PDC, α-synuclein–positive structures have been detected in the amygdala in approximately 40% of cases (7, 8) and in the cerebellum in more than 60% of cases (9). In this report, we examined phosphorylated α-synuclein immunoreactivity in the brains and spinal cords from 10 patients with ALS/PDC from the Kii Peninsula (Kii ALS/PDC) and analyzed biochemical aspects of α-synuclein from 1 patient.

MATERIALS AND METHODS

Cases

We examined 10 patients with neuropathologically verified Kii ALS/PDC (mean age, 69.1 years; range, 60–77 years). Demographic features and clinical manifestations are listed in Table 1. This study was approved by the ethics committee of Mie University Graduate School of Medicine. Informed consent was obtained from the patients or their families.

Neuropathology and Immunohistochemistry

The brains and spinal cords were fixed in formalin solution for 2 to 3 weeks. The brains were sliced into coronal sections and the spinal cords were sliced axially. Paraffin-embedded samples were cut into 9-μm-thick sections for hematoxylin and eosin, Klüver-Barrera, and Gallyas-Braak staining. All histologic samples showed numerous NFTs

TABLE 1. Clinical Data

Case No.	Age, y	Sex	Duration of Illness, y	Phenotype		
				A	P	D
1	70	F	13	+	−	−
2	63	F	5	+	−	−
3	66	F	3	+	−	−
4	65	M	3	+	−	+
5	77	M	7	+	−	+
6	70	F	8	+	+	+
7	60	F	7	+	+	+
8	76	F	6	+	+	+
9	70	F	14	−	+	+
10	74	M	6	−	+	+

A, Amyotrophic lateral sclerosis; P, parkinsonism, D, dementia; F, female; M, male; −, absent; +, present.

without senile plaques. Nerve cell loss was chiefly in the temporal cortex, frontal cortex, and the nuclei of the brainstem. Loss of anterior horn cells and degeneration of pyramidal tracts were common features.

Six-micrometer-thick sections were prepared for immunohistochemical studies. Immunostaining was performed using the avidin-biotin-peroxidase complex (ABC) method with a Vectastain ABC kit (Vector Laboratories, Burlingame, CA). The antibodies used and their dilutions were as follows: anti-phosphorylated α-synuclein antibody specifically recognizes phosphorylation at Ser-129 (PSer129, 1:5000; monoclonal; Wako, Osaka, Japan) and anti–phosphorylated tau antibody (AT8, 1:100; monoclonal, Innogenetics, Ghent, Belgium). Regions selected for evaluation are shown in Table 2. To evaluate the phosphorylated α-synuclein–positive structures and phosphorylated tau-positive structures, scores ranging from (−) to (+++) were assigned according to the number of structures in the area of maximum density. Phosphorylated α-synuclein–positive and phosphorylated tau-positive neurons were counted in 100× microscopic fields. Densities of phosphorylated α-synuclein–positive were scored as follows: −, 0; ±, 1; +, 2 to 5; ++, 6 to 10; +++, more than 10/field. Densities of phosphorylated tau-positive neurons were scored as follows: −, 0; +, 1 to 10; ++, 11 to 20; +++, more than 20/field. Colocalization of phosphorylated α-synuclein and phosphorylated tau was determined in sections double-labeled with PSer129 antibody and AT8 antibody using immunofluorescent substrate (Alexa Fluor 488 and 546; Life Technologies, Carlsbad, CA).

Western Blot

Sarkosyl-insoluble α-synuclein was extracted from the hippocampus of case 10. Sarkosyl-insoluble α-synuclein was prepared as previously described (10, 11) with slight modifications. Briefly, frozen brain tissue samples were homogenized in a 20-fold volume of buffer A (10 mmol/L Tris, pH 7.5, 1 mmol/L EGTA, 1 mmol/L dithiothreitol, 10% sucrose) containing 1% Triton X-100, incubated for 30 minutes at 37°C and spun at 100,000 × *g* for 30 minutes at 25°C. The resultant pellets were subsequently homogenized in buffer A containing 1% sarkosyl, incubated at 37°C for 30 minutes, and centrifuged 100,000 × *g* for 30 minutes. The sarkosyl-insoluble pellet was homogenized in 4 volumes of buffer A containing 1% CHAPS and spun at 100,000 × *g* for 20 minutes. The pellet was sonicated in 1 volume of 8 mol/L urea and spun at 100,000 × *g* for 20 minutes. The supernatant was mixed with an equal volume of 2× SDS sample buffer and treated at 100°C for 3 minutes. Aliquots of the samples were separated on a 10% or 15% sodium dodecyl sulfate (SDS)–polyacrylamide gel and transferred to a polyvinylidene difluoride membrane. The membrane was then probed with PSer129 (1:2000) and phosphorylation-independent anti–α-synuclein antibody (Syn 102: mouse monoclonal antibody, epitope location on α-synuclein residues 131–140) (12).

In vitro ubiquitination of α-synuclein was performed as previously described (12) with minor modifications. Briefly, 20 μg of human recombinant α-synuclein and 2 μg of ubiquitin (derived from bovine blood cells) or methylated ubiquitin were incubated with an ubiquitin ligase fraction (Fraction II) from rabbit reticulocytes at 37°C for 2 hours in a buffer containing 50 mmol/L Tris-HCl (pH 9.0), 2 mmol/L ATP, 5 mmol/L $MgCl_2$, and 1 mmol/L dithiothreitol. The conjugation reaction was stopped by boiling the samples in an equal volume of SDS sample buffer followed by separation of the components by SDS–polyacrylamide gel electrophoresis. To examine the ubiquitinated state of α-synuclein, we compared the mobilities of α-synuclein derived from Kii ALS/PDC, ubiquitinated, and unubiquitinated recombinant α-synuclein by SDS–polyacrylamide gel electrophoresis using anti-ubiquitin monoclonal antibody 1510 (anti-Ub 1510) (12). Ubiquitinated and unubiquitinated recombinant α-synuclein were identified by labeling with PSer129 and Syn102.

RESULTS

A representative image of a neuron with LBs and adjacent neurons with NFTs is shown in Figure 1A. Various types of phosphorylated α-synuclein–positive structures, including neuronal cytoplasmic inclusions and LBs (Fig. 1B), Lewy neurites (Fig. 1C), and glial cytoplasmic inclusions (Fig. 1D), were found in all ALS/PDC cases. There were no neuronal intranuclear inclusions. Phosphorylated α-synuclein–positive neurons were found in 8 (80%) of the 10 cases. Phosphorylated α-synuclein–positive neurons were

TABLE 2. Topographical Distribution of α-Synuclein–Positive Neurons and Tau-Positive Neurons

			Case 1	Case 2	Case 3	Case 4	Case 5	Case 6	Case 7	Case 8	Case 9	Case 10
Diagnosis:			**ALS**	**ALS**	**ALS**	**ALS With D**	**ALS With D**	**PDC**	**PDC**	**PDC**	**PDC**	**PDC**
Sex			**F**	**F**	**F**	**M**	**M**	**F**	**F**	**F**	**F**	**M**
Age, y			**70**	**63**	**66**	**65**	**77**	**70**	**60**	**76**	**70**	**75**
Frontal cortex BA8/9		Tau	−	+	+	++	NA	++	+	++	+	−
		αS	−	−	NA	−	−	−	−	−	−	−
Cingulate gyrus BA24		Tau	−	+	NA	+	NA	NA	−	+	++	−
		αS	−	−	NA	−	−	−	−	−	−	−
Insula		Tau	+	++	+	++	+	++	++	+	++	+
		αS	−	−	NA	−	−	−	−	−	−	+
Parietal cortex BA40		Tau	NA	NA	NA	+	NA	NA	NA	+	−	+
		αS	−	−	NA	−	NA	NA	NA	NA	−	±
Temporal cortex BA21		Tau	+	+++	+	+	+++	+++	++	++	++	+
		αS	−	−	−	−	−	−	−	±	−	+
Hippocampus (Ammon horn)		Tau	+++	+++	+	+++	+++	+++	+++	+++	+++	+++
		αS	−	−	−	−	−	−	++	+	−	++
Meynert nucleus		Tau	+	+	NA	++	++	++	+++	NA	+	+
		αS	−	−	NA	−	−	−	+++	NA	−	−
Caudate nucleus		Tau	−	+	NA	+	+	NA	±	+	+	−
		αS	−	−	NA	−	−	−	+	−	+	−
Putamen		Tau	+	++	NA	+	+	NA	±	+	+	+
		αS	−	−	NA	−	−	−	+	−	−	−
Pallidum		Tau	−	+	NA	+	+	NA	±	NA	+	+
		αS	−	−	NA	−	−	−	+	NA	−	−
Transentorhinal cortex BA28		Tau	++	+++	+	++	++	+++	+++	+++	++	+++
		αS	−	−	−	−	−	−	+	++	−	±
Motor cortex		Tau	NA	+	NA	+	+	++	+	+	++	NA
		αS	NA	NA	NA	−	−	−	−	−	−	−
Thalamus		Tau	−	+	+	+	−	NA	++	+	++	+
		αS	−	NA	NA	−	−	NA	−	NA	−	−
Subthalamic nucleus		Tau	−	+	NA	+	NA	NA	NA	+	+	+
		αS	−	NA	NA	−	NA	NA	NA	NA	±	±
Amygdala		Tau	+++	+++	+++	+++	+++	++	+++	++	+++	+++
		αS	−	−	−	+	+	+	++	+	±	+++
Parahippocampus		Tau	+++	+++	+	++	+++	+++	+++	+++	+++	+++
		αS	−	−	−	−	−	−	++	+	−	+++
Cerebellum	Molecular layer	Tau	−	−	−	−	−	−	+	−	−	−
		αS	−	−	−	−	−	−	−	−	−	−
	Dentate nucleus	Tau	−	+	−	+	+	+	++	+	+++	+
		αS	−	−	−	+	−	−	−	+	−	−
	White matter	Tau	−	−	−	−	−	+	−	−	+	−
		αS	−	−	−	−	−	−	−	±	−	−
Midbrain	Substantia nigra	Tau	−	+	+	+	+	++	+	+++	+++	++
		αS	++	−	−	+	−	−	++	+	−	++
	Periaqueductal gray	Tau	+	+++	+++	+++	+	+	++	+++	+++	+++
		αS	+	−	−	+	−	−	+++	++	−	++
Pons	Locus coeruleus	Tau	+	++	+	+	+	+	+	+++	+++	+++
		αS	+++	−	−	+++	−	−	−	+++	−	+++
	Raphe nuclei	Tau	+	+	+	+	+	+	+	+	+++	+++
		αS	−	−	−	+	−	−	−	+++	−	++
	Pontine nucleus	Tau	−	−	−	−	−	−	−	+	+++	−
		αS	−	−	−	−	−	−	−	−	−	−

(Continued on next page)

TABLE 2. *(Continued)*

			Case 1	Case 2	Case 3	Case 4	Case 5	Case 6	Case 7	Case 8	Case 9	Case 10
Diagnosis:			ALS	ALS	ALS	ALS With D	ALS With D	PDC	PDC	PDC	PDC	PDC
Sex			F	F	F	M	M	F	F	F	F	M
Age, y	70		63	66	65	77	70	60	76	70	75	
Medulla	Dorsal nucleus of vagus nerve	Tau	+	+	−	−	−	+	−	−	−	+
		αS	+	−	−	+++	−	−	−	−	−	+++
	Hypoglossal nucleus	Tau	+	±	−	−	−	+	+	−	+	−
		αS	−	−	−	−	−	−	−	−	−	+
	Inferior olivary nucleus	Tau	−	−	−	−	−	+	+	−	+	++
		αS	−	−	−	−	−	−	−	−	−	+
spinal cord	Ventral horn	Tau	−	−	−	NA	−	−	+	+	++	+
		αS	−	−	−	NA	−	−	−	++	−	+
	Intermediolateral nucleus	Tau	−	−	+	NA	−	−	+	+	+	−
		αS	±	−	−	NA	−	−	±	−	−	+++

α-Synuclein (αS)–positive neurons were counted in microscope fields at a magnification of 100× and the density of α-synuclein positive neurons was scored as follows: −, 0; ±, 1; +, 2 to 5: ++, 6 to 10; +++, more than 10. The density of tau-positive neurons was scored at a magnification of 100× as follows: to , 0; +, 1 to 10; ++, 11 to 20; +++, more than 20.

mainly detected in the amygdala (70%); substantia nigra, periaqueductal gray (50%); locus coeruleus (40%); and hippocampus, transentorhinal cortex, parahippocampus, raphe nucleus, dorsal vagal nucleus, and intermediolateral nucleus of the spinal cord (30%) (Table 2). There were no phosphorylated α-synuclein–positive structures in the molecular layer of the cerebellum in any of the 10 cases. Tau-positive neurons were abundant in most areas examined. Phosphorylated α-synuclein–positive neurons outnumbered tau-positive neurons in the substantia nigra, locus coeruleus, and dorsal nucleus of the vagus nerve in a few patients, and periaqueductal gray, raphe nucleus, spinal ventral horn, and spinal intermediolateral nucleus in only 1 or 2 patients (Table 2). Semiquantitative evaluation suggested that the densities of

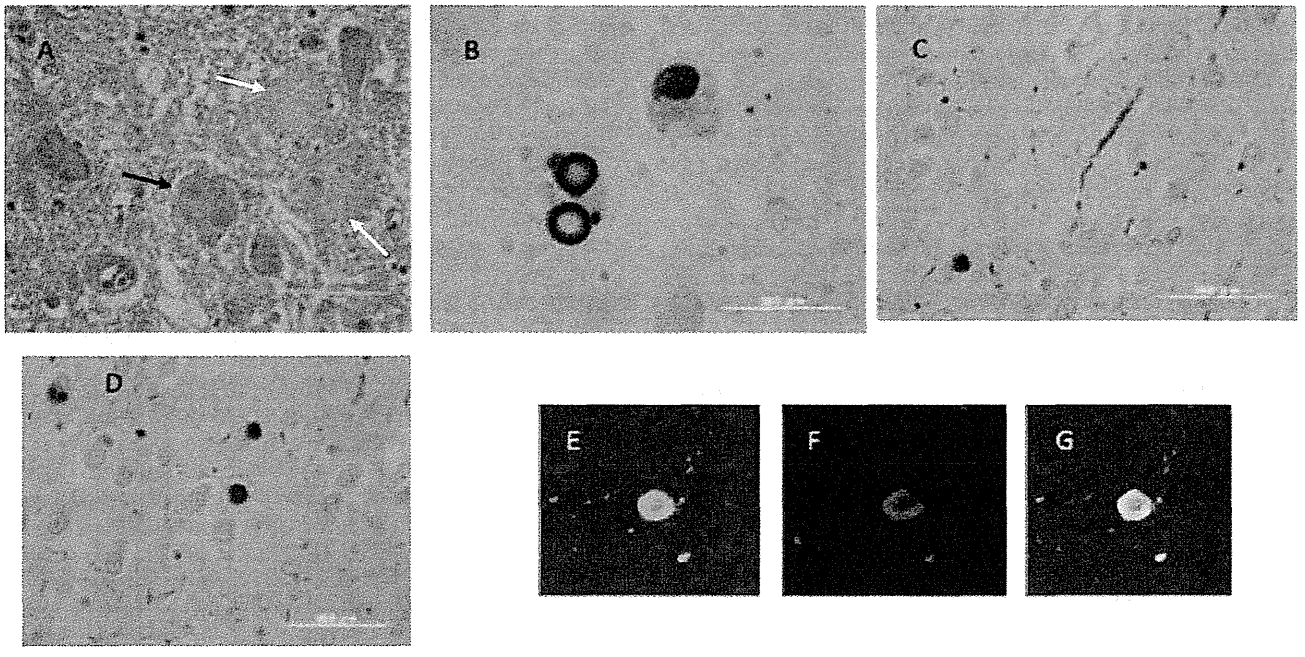

FIGURE 1. Hematoxylin and eosin staining, immunostaining using an antibody against phosphorylated α-synuclein (PSer129), and double immunofluorescence with PSer129 and anti-phosphorylated tau (AT8) antibodies. **(A)** Lewy bodies (LBs) (black arrow) and neurofibrillary tangles (NFTs) (yellow arrows) in the locus coeruleus (hematoxylin and eosin stain). **(B)** LBs and cytoplasmic round inclusion in the locus coeruleus (PSer129). **(C)** Lewy neurites in the amygdala (PSer129). **(D)** Glial cytoplasmic inclusion in the amygdala (PSer129). **(E–G)** Double immunofluorescence labeling showing the coexistence of α-synuclein (PSer129, Alexa 488: green) **(E)**, tau (AT8, Alexa 546: red) **(F)**, and their merged image **(G)**.

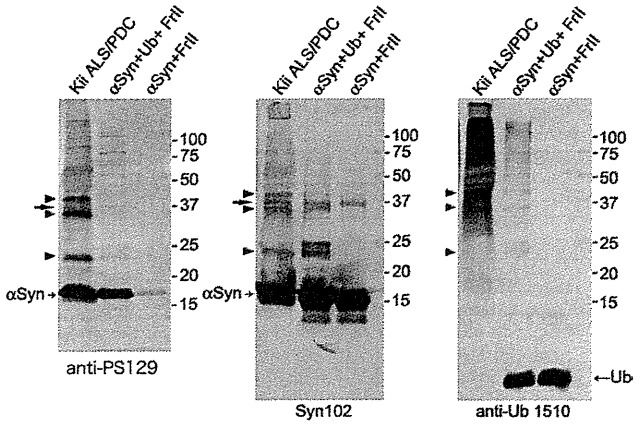

FIGURE 2. Sarkosyl-insoluble fractions from case 10 with Kii amyotrophic lateral sclerosis/parkinsonism dementia complex (ALS/PDC), ubiquitinated recombinant α-synuclein (αSyn + Ub + Frll), and nonubiquitinated recombinant α-synuclein (αSyn + Frll). Samples were immunoblotted with a phosphorylation-dependent anti–α-synuclein antibody (anti-PSer129) (PS129), a phosphorylation-independent anti–α-synuclein antibody (Syn 102), and an anti-ubiquitin (Ub) antibody (anti-Ub 1510). Note that 24-, 32-, and 40-kDa bands are detected in the Kii ALS/PDC brain and αSyn + Ub + Frll with anti-PSer129, Syn 102, and anti-Ub 1510 (arrowheads). Arrow indicates an α-synuclein dimer, which was also detected in αSyn + Frll.

phosphorylated α-synuclein–positive neurons were not related to age or duration of illness but to the densities of tau-positive neurons. Colocalization of phosphorylated α- synuclein and phophorylated tau was observed in many neuronal cytoplasmic inclusions and neuropil threads in the amygdala, substantia nigra, periaqueductal gray, locus coeruleus (Figs. 1E–G), hippocampus, transentorhinal cortex, and parahippocampus.

Immunoblots of sarkosyl-insoluble fractions extracted from the brain of a Kii ALS/PDC patient showed a few α-synuclein–immunoreactive bands. The major immunoreactive band with an apparent molecular mass of 17 kDa and minor 24-, 32-, and 40-kDa bands migrating at a higher molecular mass range on the Tris–glycine gel system were immunoreactive with PSer129 and Syn102. The higher molecular mass of phosphorylated α-synuclein-related polypeptides suggested ubiquitination compared with recombinant α-synuclein, which was incubated with the ubiquitin ligase fraction with or without ubiquitin (Fig. 2), as previously reported in other synucleinopathies (12).

DISCUSSION

α-Synuclein–positive pathology has been identified in a variety of disorders with extensive tau pathology including sporadic Alzheimer disease (13, 14), familial Alzheimer disease (15), DLB (16), familial DLB (17), familial Parkinson disease associated with the α-synuclein A53T mutation (18), Down syndrome (19), neurodegeneration with brain iron accumulation (20–22), and Guam PDC (7–9). Colocalization of tau and α-synuclein was variable in these diseases. For example, extensive colocalization of tau and α-synuclein was reported in DLB (16) and familial DLB (17); the co-occurrence of tau and α-synuclein was variable in Guam PDC (7, 8).

In the present study, the frequency, distribution, and morphology of α-synuclein deposits are described in the brains and spinal cords of patients with Kii ALS/PDC for the first time. α-Synuclein deposits were observed mainly in the limbic system and brainstem; α-synuclein was phosphorylated and ubiquitinated. Tau-positive neurons were more abundant than α-synuclein–positive neurons in most areas examined, and there was extensive colocalization of tau and α-synuclein.

Although Kii ALS/PDC and Guam ALS/PDC share a number of clinical and neuropathologic features, it remains unclear whether they are identical. Yamazaki et al (7) examined α-synuclein–positive intraneuronal inclusions in the motor cortex, medial temporal lobe, and brainstem of 13 patients with Guam PDC using antibodies against non-phosphorylated α-synuclein; they found that 7 (54%) of 13 PDC patients showed α-synuclein–positive inclusions in at least 1 region of the brain. The authors concluded that the amygdala was most affected by α-synuclein pathology, in which α-synuclein was frequently colocalized with tau. Forman et al (8) reported that α-synuclein pathology of the amygdala in Guam ALS/PDC was present in 37% of 19 patients with PDC, but absent in patients with ALS, preclinical PDC, early PDC/ALS, clinical (pathology pending) PDC, PDC/ALS, and control Chamorro patients. The α-synuclein aggregates rarely colocalized within neurons harboring NFTs. On the basis of these findings, the authors suggested a possible interaction between tau and α-synuclein and tau deposits preceding α-synuclein deposits. Sebeo et al (9) reported that numerous α-synuclein–immunoreactive spherical structures in the molecular layer of the cerebellum were observed in 63.6% of Guam PDC patients. These structures were seen exclusively in patients showing α-synuclein pathology in the amygdala, and were much more pronounced in the hemisphere than in the vermis and were associated with Purkinje cells and Bergmann glia cells.

We found that in Kii ALS/PDC, α-synuclein pathology in the amygdala was absent in patients with ALS but was present in ALS patients with dementia and PDC. These results suggest that the α-synuclein pathology in the amygdala may have been induced by tau deposition and may be related to dementia in ALS/PDC. Because α-synuclein inclusions are not found in every brain with other tauopathies, tau in ALS/PDC cases might accelerate α-synuclein aggregation. The combination of misfolded α-synuclein and tau that occurs in ALS/PDC might promote cytotoxic protofibrils and accelerate protein deposits (23). We carefully searched the cerebellum of Kii ALS/PDC patients for similar α-synuclein–positive structures in the molecular layer but failed to find α-synuclein–positive pathology. In general, neuronal cell loss and tau deposits in the molecular layer are exceptional in Kii ALS/PDC. The cause of this discrepancy in α-synuclein pathology in the cerebellum between Guam ALS/PDC and Kii ALS/PDC might be clarified by using the same antibody and identical staining protocols in further studies.

In summary, α-synuclein–positive structures were common in both ALS and PDC and were mainly distributed

in the brainstem and limbic system. The amygdala was the most affected structure in Kii ALS/PDC. The interaction between tau and α-synuclein might modify the pathogenesis of Kii ALS/PDC.

ACKNOWLEDGMENTS

The authors thank Dr T. Iwatsubo, Department of Neuropathology, University of Tokyo, for providing anti–α-synuclein antibody. The authors also thank Hisami Akatsuka for her special technical assistance in tissue preparation for histopathology.

REFERENCES

1. Hirano A, Malamud N, Elizan TS, et al. Amyotrophic lateral sclerosis and parkinsonism-dementia complex on Guam. Further pathologic studies. Arch Neurol 1966;15:35–51
2. Shiraki H, Yase Y. Amyotrophic lateral sclerosis in Japan. In: Vinken PJ, Bruyn GW, Klawans HL, eds. *Handbook of Clinical Neurology*. Amsterdam, the Netherlands: North Holland Publishing Company, 1975:353–419
3. Kuzuhara S, Kokubo Y, Sasaki R, et al. Familial amyotrophic lateral sclerosis and parkinsonism-dementia complex of the Kii peninsula of Japan: Clinical and neuropathological study and tau analysis. Ann Neurol 2001;49:501–11
4. Mimuro M, Kokubo Y, Kuzuhara S. Similar topographical distribution of neurofibrillary tangles in amyotrophic lateral sclerosis and parkinsonism-dementia complex in people living in the Kii peninsula of Japan suggests a single tauopathy. Acta Neuropathol 2007;113:653–58
5. Spillantini M, Schmidt M, Lee V-Y, et al. α-Synuclein in Lewy bodies. Nature 1997;388:839–40
6. Wakabayashi K, Yoshimoto M, Tsuji S, et al. α-Synuclein immunoreactivity in glial cytoplasmic inclusions in multiple system atrophy. Neurosci Lett 1998;249:180–82
7. Yamazaki M, Arai Y, Baba M, et al. α-Synuclein inclusions in amygdala in the brains of patients with the parkinsonism-dementia complex of Guam. J Neuropathol Exp Neurol 2000;59:585–91
8. Forman MS, Schmidt ML, Kasturi S, et al. Tau and α-Synuclein pathology in amygdala of parkinsonism-dementia complex patients of Guam. Am J Pathol 2002;160:1725–31
9. Sebeo J, Hof PR, Perl DP. Occurrence of alpha-synuclein pathology in the cerebellum of Guamanian patients with parkinsonism-dementia complex. Acta Neuropathol 2004;107:497–503
10. Miake H, Mizusawa H, Iwatsubo T, et al. Biochemical characterization of the core structure of alpha-synuclein filaments. J Biol Chem 2002;277:19213–19
11. Fujiwara H, Hasegawa M, Dohmae N, et al. alpha-Synuclein is phosphorylated in synucleinopathy lesions. Nat Cell Biol 2002;4:160–64
12. Hasegawa M, Fujiwara H, Nonaka T, et al. Phosphorylated α-Synuclein is ubiquitinated in α-Synuclein lesions. J Biol Chem 2002;277:49071–76
13. Hamilton RL. Lewy bodies in Alzheimer's disease: A neuropathological review of 145 cases using α-Synuclein immunohistochemistry. Brain Pathol 2000;10:378–84
14. Kazee AM, Han LY. Cortical Lewy bodies in Alzheimer's disease. Arch Pathol Lab Med 1995;119:448–53
15. Lippa CF, Fujiwara H, Mann DM, et al. Lewy bodies contain altered α-Synuclein in brains of many familial Alzheimer's disease patients with mutations in presenilin and amyloid precursor protein genes. Am J Pathol 1998;153:1365–70
16. Iseki E, Togo T, Suzuki T, et al. Dementia with Lewy bodies from the perspective of tauopathy. Acta Neuropathol 2003;105:265–70
17. Clarimon J, Molina-Porcel L, Gomez-Isla T, et al. Early-onset familial Lewy body dementia with extensive tauopathy: A clinical, genetic, and neuropathological study. J Neuropathol Exp Neurol 2009;68:73–82
18. Giasson BI, Forman MS, Higuchi M, et al. Initiation and synergistic fibrillization of tau and alpha-synuclein. Science 2003;300:636–40
19. Lippa CF, Schmidt ML, Lee VM-Y, et al. Antibodies to α-synuclein detect Lewy bodies in many Down's syndrome brains with Alzheimer's disease. Ann Neurol 1999;45:353–57
20. Hayashi S, Akasaki Y, Morimura Y, et al. An autopsy case of late infantile and juvenile neuroaxonal dystrophy with diffuse Lewy bodies and neurofibrillary tangles. Clin Neuropathol 1992;11:1–5
21. Wakabayashi K, Fukushima T, Koide R, et al. Juvenile-onset generalized neuroaxonal dystrophy (Hallervorden-Spatz disease) with diffuse neurofibrillary and Lewy body pathology. Acta Neuropathol 2000;99:331–36
22. Saito Y, Kawai M, Inoue K, et al. Widespread expression of α-Synuclein and tau immunoreactivity in Hallervorden-Spatz syndrome with protracted clinical course. J Neurol Sci 2000;177:48–59
23. Giasson BI, Forman MS, Higuchi M, et al. Initiation and synergistic fibrillization of tau and alpha-Synuclein. Science 2003;300:636–40

Journal of Histochemistry & Cytochemistry 60(10) 761–769

DOI: 10.1369/0022155412456379
http://jhc.sagepub.com
SAGE

Enhanced Antigen Retrieval of Amyloid β Immunohistochemistry: Re-evaluation of Amyloid β Pathology in Alzheimer Disease and Its Mouse Model

Hideaki Kai, Ryong-Woon Shin, Koichi Ogino, Hiroyuki Hatsuta, Shigeo Murayama, and Tetsuyuki Kitamoto

Department of Neurological Science, Tohoku University Graduate School of Medicine, Sendai, Japan (HK,R-WS,TK); Qs' Research Institute, Otsuka Pharmaceutical Co. Ltd., Tokushima, Japan (KO); and Department of Neuropathology (The Brain Bank for Aging Research), Tokyo Metropolitan Geriatric Hospital & Institute of Gerontology, Tokyo, Japan (HH,SM).

Summary

Senile plaques, extracellular deposits of amyloid β peptide (Aβ), are one of the pathological hallmarks of Alzheimer disease (AD). As the standard immunohistochemical detection method for Aβ deposits, anti-Aβ immunohistochemistry combined with antigen retrieval (AR) by formic acid (FA) has been generally used. Here, we present a more efficient AR for Aβ antigen. On brain sections of AD and its mouse model, a double combination of either autoclave heating in EDTA buffer or digestion with proteinase K plus FA treatment reinforced Aβ immunoreactivity. A further triple combination of digestion with proteinase K (P), autoclave heating in EDTA buffer (A), and FA treatment (F), when employed in this order, gave a more enhanced immunoreactivity. Our PAF method prominently visualized various forms of Aβ deposits in AD that have not been clearly detected previously and revealed numerous minute-sized plaques both in AD and the mouse model. Quantification of Aβ loads showed that the AR effect by the PAF method was 1.86-fold (in the aged human brain) and 4.64-fold (in the mouse brain) higher than that by the FA method. Thus, the PAF method could have the potential to be the most sensitive tool so far to study Aβ pathology in AD and its mouse model. (J Histochem Cytochem 60:761–769, 2012)

Keywords

Alzheimer disease, amyloidβ, antigen retrieval, APP-SL mouse, autoclave heating, formic acid, immunohistochemistry, minute plaque, PAF method, proteinase K

Senile plaques (SPs) and neurofibrillary tangles (NFTs) are two pathological hallmarks that characterize brains afflicted with Alzheimer disease (AD). SPs are extracellular deposits of amyloid β peptide (Aβ) mainly consisting of 40 and 42 residues, which are cleavage products of the amyloid precursor proteins (APPs) (Masters et al. 1985; Kang et al. 1987; Iwatsubo et al. 1994). Aβ is a hydrophobic self-aggregating peptide, and the aggregation of soluble Aβ monomers leads to the composition of insoluble fibrillar polymers, Aβ fibrils. NFTs are intracellular aggregated bundles of a hyperphosphorylated form of the microtubule-associated protein tau (Lee et al. 1991; Ballatore et al. 2007).

Although it is not yet completely elucidated whether SPs and NFTs are the causes or the results of AD onset, the aggregation of Aβ is believed to be implicated in the upper stream of the cascade of AD pathogenesis as a pivotal player in the development of dementia: the amyloid hypothesis (Selkoe 1991; Hardy and Higgins 1992; Hardy and Selkoe 2002). Therefore, the detection of SPs or Aβ deposits with high specificity and sensitivity is essential for elucidating the roles of

Received for publication, June 2, 2012; accepted, June 30, 2012.

Supplementary material for this article is available on the *Journal of Histochemistry & Cytochemistry* Web site at http://jhc.sagepub.com/supplemental.

Corresponding Author:
Ryong-Woon Shin, Department of Neurological Science, Tohoku University Graduate School of Medicine, 2-1 Seiryo-machi, Sendai 980-8575, Japan.
Email: rwshin@med.tohoku.ac.jp

parenchymal Aβ deposition and its implication for the pathogenesis of AD as well as its pathological diagnosis. In 1987, our attempt to attain sensitive Aβ immunohistochemistry (IHC) results on formalin-fixed paraffin-embedded (FFPE) tissue sections led to the development of Aβ antigen retrieval (AR) by formic acid (FA) (Kitamoto et al. 1987). This straightforward method dramatically enhances the detection level of Aβ deposits in the AD brain, and since then, anti-AβIHC coupled with FA treatment has been the standard method in the field of Aβ pathology. There is no guarantee, however, that this method can expose all of the existing Aβ deposits without the remains, and we consider that there might be room for improvement of the AR technique. In fact, we had a chance to find irregular and larger forms of Aβ staining, known as fleecy amyloid deposits (Thal et al. 1999), which appear different from the usual SPs in the entorhinal cortex of some AD cases. These structures of Aβ aggregates stained too faintly to be recognized clearly, and we thought that the AR mediated by FA was not efficient enough to detect these Aβ structures. Thus, we tackled the development of a new AR method with a higher efficiency than the conventional FA method. We could substantially improve Aβ IHC by applying two other AR procedures prior to FA treatment. This new AR method enhanced the detection level of numerous SPs and various Aβ deposits that have not been clearly detected by the conventional method and provides a tool to uncover new aspects of Aβ pathology in AD and its mouse models.

Materials and Methods

Brain Specimens

Human brain specimens were derived from patients with AD (n=11; age range = 63–79 years), non-AD aged individuals with Aβ plaques (n=4; age range = 63–77 years), and negative controls for Aβ IHC, who have no family history of AD, including non-AD aged individuals without Aβ plaques (n=10; age range = 64–94 years) and healthy young individuals (n=6; age range = 21–38 years). For quantification of the Aβ loads, we examined a series of aged human individuals with varying degrees of the Aβ burden (n=54; age range = 69–94 years). As transgenic AD mouse models, we used the APP–Swedish/London (SL) lines 7–5 and 7–9, which overexpress human $APP_{Swe/Lon}$ harboring both the Swedish- and London-type mutations. The levels of APP, Aβ40, and Aβ42 in the brain tissues of the mice of line 7–5 are higher than the corresponding levels in the mice of line 7–9 (Shin et al. 2007). The outline of the ages of each of them is as follows: line 7–5 of APP-SL mice aged 6 months (n=3), 8 months (n=8), 9 months (n=2), 10 months (n=2), 11 months (n=1), 12 months (n=4), 13 months (n=6), 15 months (n=1), 16 months (n=5), and 18 months (n=1); line 7–9 of APP-SL mice aged 3 months (n=3), 6 months (n=3), 9 months (n=3), 12 months (n=2), 13 months (n=3), 15 months (n=1), 16 months (n=2), 18 months (n=2), 19 months (n=1), and 36 months (n=1). The fixation time of brains was 7–13 days with 20% buffered formalin in humans and 3–4 days with 10% buffered formalin in mice. The use of human brains for this work was approved by the Institutional Review Board of Tohoku University Graduate School of Medicine and Tokyo Metropolitan Geriatric Hospital & Institute of Gerontology, and all the animal experiments were done according to the Guidelines for Animal Care and Use at Otsuka Pharmaceutical Co. Ltd.

AR Procedures

FA pretreatment has been the standard AR method for Aβ IHC. In FA pretreatment, brain tissue sections were incubated in 98% FA (Wako Pure Chemical Industries; Osaka, Japan) for 5 min at room temperature. A challenging trial to largely improve the FA method was performed by combining and applying other AR methods prior to FA treatment. The other AR methods used in this study include heating that employs immersion of tissue sections in 10 mM EDTA (pH 3.0, pH 6.0, and pH 10.0) (Murayama et al. 1999), 0.05% citraconic anhydride (pH 3.0, pH 7.4, and pH 10.0) (Namimatsu et al. 2005), and 0.1 M sodium citrate (pH 3.0, pH 7.2, and pH 10.0) (Bataille et al. 2006) solutions, and distilled water (DW) (pH 3.0 adjusted with hydrochloric acid, pH 7.1, and pH 10.0 adjusted with sodium hydroxide), using an autoclave at 105C or 121C for 10 min (Shin et al. 1991) or using a microwave oven at 90C intermittently but for a total of about 10 min; the proteolytic digestion of tissue sections was performed at 37C for 30 min with 1.0 μg/ml of proteinase K (PK) (Wako Pure Chemical Industries) and 100.0 μg/ml trypsin (Wako Pure Chemical Industries) dissolved in 1.0 mM $CaCl_2$/50 mM Tris buffer (pH 7.6). After each AR treatment, these sections were washed with tap water for at least 5 min and then incubated in DW for at least 5 min.

Immunostaining

With pretreatment of various combinations of the AR methods, immunostaining was performed as described (Murayama et al. 1999; Shin et al. 2007) using the polyclonal Aβ antibody 4702 (1:1500) (Shin et al. 2007) and monoclonal Aβ antibodies 6E10 (1:2000–4000; Senetek, Maryland Heights, MO) and 4G8 (1:20,000; Senetek). The concentrations of these antibodies were optimized in consideration of both the immunoreactivity and backgrounds of IHC. Brain sections were incubated with primary antibodies in 0.1% Tween-20/Tris-buffered saline (Tris, 50 mM; NaCl, 500 mM; pH 7.6) containing 5% nonfat dried milk for about 15 hr at room temperature. To exclude nonspecific staining unrelated to these polyclonal and monoclonal antibodies, immunostaining was performed with

omission of the antibodies but with all other procedures unchanged in some experiments. Secondary antibodies of EnVision+ system HRP-labeled polymer (Dako; Glostrup, Denmark) were used for the detection of antigen primary mouse or rabbit antibody complexes by diaminobenzidine (DAB). The incubation of the secondary antibodies was for about 1 hr at room temperature. The immunostained brain sections were counterstained with hematoxylin.

Microscopes

The photomicrographs of human and murine samples were captured by an Axiophot2 microscope (Carl Zeiss; Oberkochen, Germany) with Axio Vision version 4.6.3.0 software (Carl Zeiss). In quantification of the Aβ load in the hippocampus of the murine samples, the same system was used in order to assemble sequential micrographs into a single larger one. For measuring the Aβ load, aged human sample photomicrographs were captured by C9600 NanoZoomer (Hamamatsu Photonics; Hamamatsu, Japan) with NDP.view software (Hamamatsu Photonics) because this system is conveniently applicable for capturing and comparing the same regions from serial sections.

Measurement of the Area of Aβ Deposits

In the human brains, we selected three microscopic fields in the fusiform gyrus, which are adequately separated from each other and contain relatively higher Aβ loads. We photographed precisely the same fields in each serial section immunostained following the FA method or PK digestion (P), EDTA autoclaving (A), and FA treatment (F) (in that order; referred to as "PAF") method. All images were from regions of 1408 μm × 1874 μm. In the mouse brains, we selected the whole hippocampus, and its image was constructed from the photomicrographs of 872 μm × 1100 μm by using panorama module of AxioVision version 4.6.3 (Carl Zeiss). All the images were analyzed by ImageJ version 1.43 m (National Institutes of Health; Bethesda, MD) as follows: 1) each raw image was resolved into three images by the color deconvolution setting in hematoxylin and eosin and DAB; 2) the DAB color image among the three resolved images was selected for analysis; 3) the threshold value of the selected image was set to zero as the minimum value and at the optically optimum value set as the maximum value; 4) the thresholded areas of cerebral amyloid angiopathy and artifacts were excluded by selecting and filling them; 5) areas of the Aβ loads (%) to be measured were within a circle (diameter = 1408 μm), the center of which being in the middle of each image in the aged human brains, and within the circumscribed edge of the hippocampus drawn using the selection tools in the mouse brains; and 6) area fractions of the residual thresholded objects within these selections were measured.

Statistical Analyses

All the statistical analyses were performed with SPSS version 17.0 (SPSS; Chicago, IL).

Results

Development of the Enhanced AR Method for Aβ IHC

For the development of a more efficient Aβ AR method, our strategy was to modify and reinforce the retrieving effects of FA by applying other AR procedures prior to FA treatment. Such AR procedures included autoclave heating in EDTA buffer (the chelating autoclave method) (Murayama et al. 1999) and digestion with PK. With each of these AR procedures followed by FA treatment or with FA treatment alone, immunostaining using the polyclonal anti-Aβ 4702 antibody was performed on brain tissue sections derived from AD patients and APP-SL line 7–5 mice. In immunostaining using the 4702 antibody with no AR, almost no plaques were detected in the AD brains or only a few in the mouse brains (Suppl. Fig. S1). Thus, this 4702 antibody was conveniently used to easily evaluate the effectiveness of the Aβ AR methods.

Compared to the AR procedures above followed by FA treatment and FA treatment alone, both combinations of AR enhanced the Aβ immunoreactive intensity and increased the loads of Aβ plaques, albeit with low to high enhancing effects (Fig. 1A–C,E–G). However, when we applied heating to the EDTA solution, counterstaining of tissue sections with hematoxylin was remarkably thin compared with counterstaining in the FA only method. Notably, the reversed application of the two AR procedures, that is, application of FA treatment and either autoclave heating in EDTA buffer or digestion with PK in this order, showed limited and almost no enhancement, respectively, compared with the single application of FA treatment (data not shown). These results prompted us to try a triple combination of these three AR procedures. The use of the PAF method produced a remarkably stronger enhancement of Aβ immunoreactivity than the two double combinations above (Fig. 1B–D,F–H). In the triple combinations of the three AR methods in different orders other than that used in the PAF method, varying degrees of tissue damage ensued, especially in human brains. Therefore, we refrained from estimating those triple AR combinations. To confirm that this PAF method is universally applicable to Aβ IHC, we examined other Aβ antibodies including 6E10 (Fig. 2A, B, E, F) and 4G8 (Fig. 2C, D, G, H). All of these antibodies showed enhanced Aβ immunoreactivity following the PAF method compared with the FA method, albeit with varied enhancing effects. Omission of the polyclonal or monoclonal primary antibodies in Aβ IHC with the PAF method totally abolished positive immunostaining (Suppl. Fig. S2),

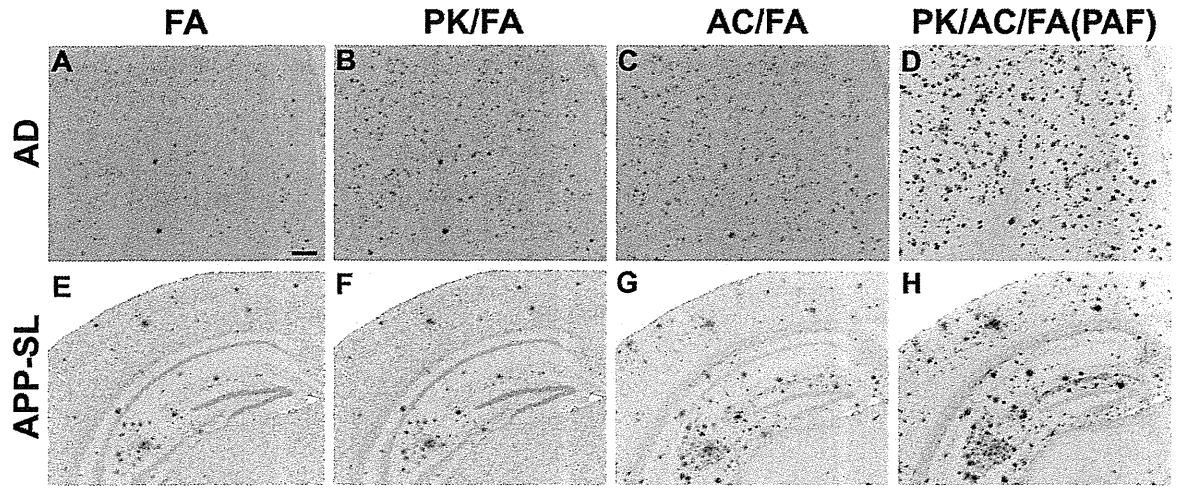

Figure 1. Enhancement of formic acid (FA)–mediated amyloid β peptide (Aβ) antigen retrieval. Serial brain tissue sections from a 74-year-old male patient with Alzheimer disease (A–D) and from a 13-month-old amyloid precursor protein–Swedish/London (APP-SL) mouse of line 7–5 (E–H) were immunostained with anti-Aβ antibody 4702 following pretreatment by FA alone (FA) (A, E); combination of digestion with proteinase K and FA (PK/FA) (B, F); combination of autoclave heating in EDTA buffer and FA (AC/FA) (C, G); and triple combination of digestion with proteinase K, autoclave heating in EDTA buffer, and FA (PK/AC/FA) (D, H). Pictures (A–D) are from the temporal cortex. Scale bar = 200 μm (A–H).

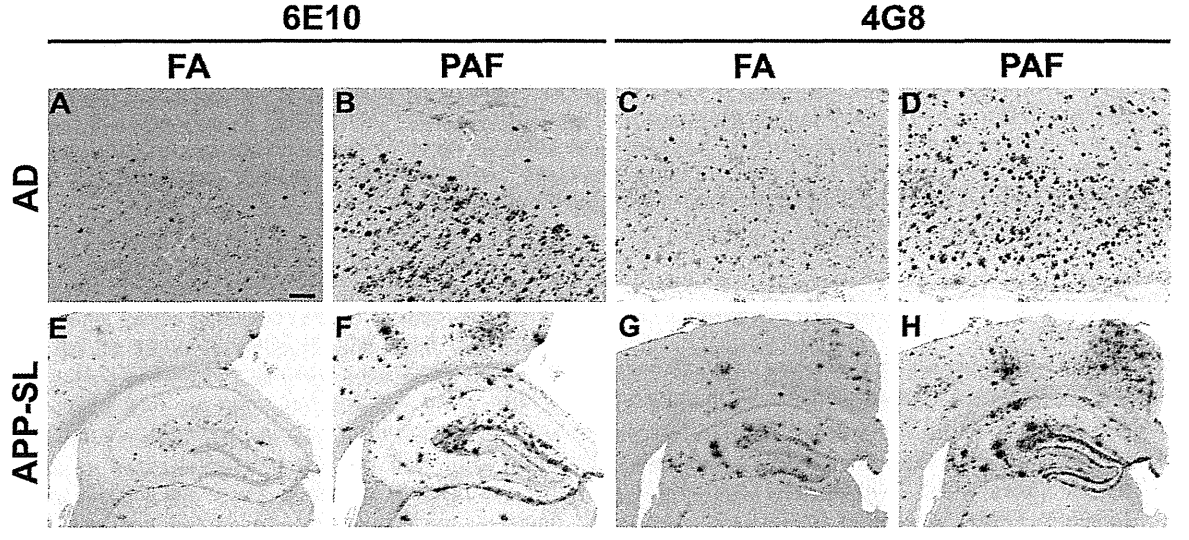

Figure 2. General application of the proteinase K digestion (P), EDTA autoclaving (A), and formic acid (FA) treatment (F) (in that order; referred to as "PAF") method in amyloid β peptide (Aβ) immunohistochemistry. Serial (A–B, C–D, E–F, G–H) brain tissue sections from a 74-year-old male patient with Alzheimer disease (the same patient as shown in Fig. 1) (A–D) and a 16-month-old (E, F) and a 15-month-old (G, H) amyloid precursor protein–Swedish/London (APP-SL) mouse of line 7–5 were immunostained with monoclonal anti-Aβ antibodies 6E10 (A, B, E, F) and 4G8 (C, D, G, H) following pretreatment by the FA (A, C, E, G) and PAF methods (B, D, F, H). Pictures are from the cingulate cortex (A, B) and the frontal cortex (C, D). Scale bar = 200 μm (A–H).

which excludes the possibility that immunoreactivity augmented and disclosed following the PAF method was due to nonspecific staining. In addition, no artifactual immunostaining was observed in the brain sections from the normal younger individuals following Aβ IHC assisted by the PAF method (Suppl. Fig. S3).

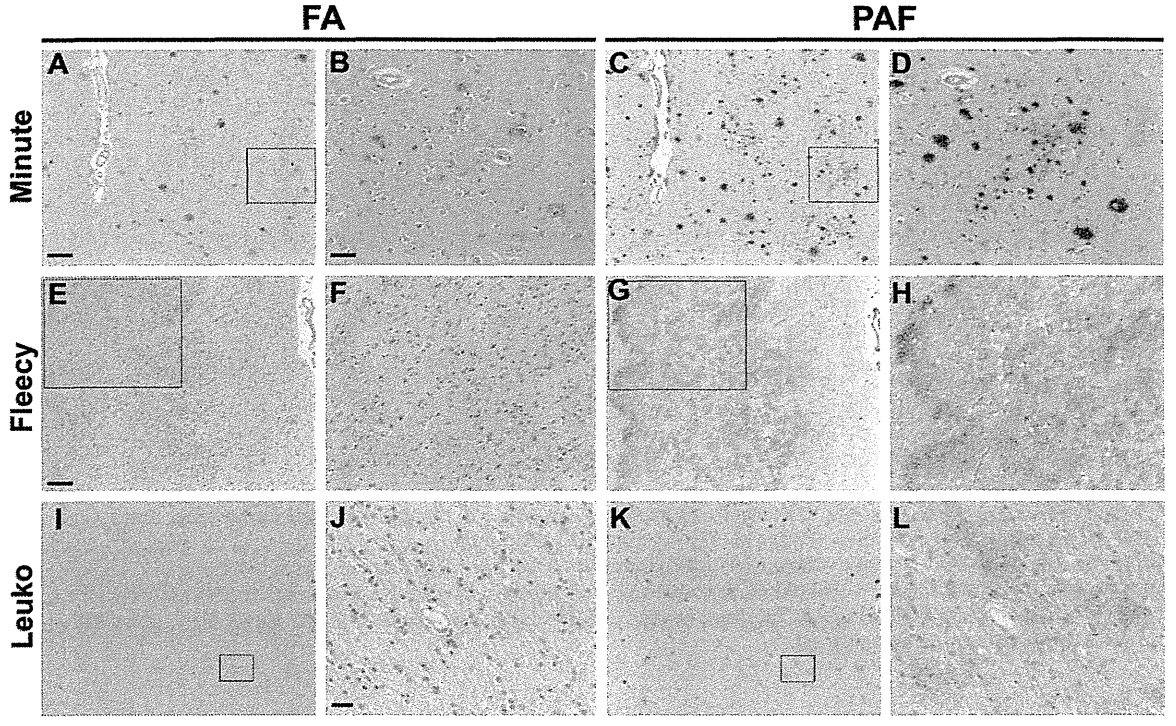

Figure 3. Amyloid β peptide (Aβ) pathology of Alzheimer disease (AD) brains enhanced by the proteinase K digestion (P), EDTA autoclaving (A), and formic acid (FA) treatment (F) (in that order; referred to as "PAF") method. Serial brain tissue sections from a 72-year-old female AD patient (the identical patient as shown in Suppl. Fig. S1A,B) (A–D), a 74-year-old male AD patient (the same patient as shown in Fig. 1) (E–H), and a 74-year-old female AD patient (I–L) were immunostained with the 4702 antibody following pretreatment by the FA (A, B, E, F, I, J) and PAF methods (C, D, G, H, K, L). Pictures are from the frontal cortex (A–D), the entorhinal cortex (E–H), and the frontal white matter (I–L). B, D, F, H, J, and L are higher magnification pictures of areas outlined by squares in A, C, E, G, I, and K, respectively. Scale bars = 200μm (A, C, I, K); 50 μm (B, D, F, H); 100μm (E, G); and 20 μm (J, L).

IHC Analysis of AD Brains by the PAF Method

Serial sections of the AD brains pretreated with either the PAF or FA method were immunostained with the anti-Aβ 4702 antibody, analyzed for pathological Aβ deposits, and compared between these two methods (Fig. 3). In the cerebral cortex and hippocampus of the sections pretreated with the PAF method, larger Aβ plaques (diameter > ~15 μm) showed immunoreactive enhancement with an enlarged robust contour, although there was no apparent increase in the number of these larger Aβ plaques. The prominent effect given by the PAF method was the disclosure of numerous minute-sized (diameter < ~15 μm) fine-granular plaques (hereafter referred to as "minute plaques") in these brain regions, which were not evidently detected by the FA method (Figs. 1A, D and 3A–D). Remarkably, the number of these minute plaques increased with elevation of the total Aβ load (data not shown). Thus, all of the AD brains examined by the PAF method contained a much higher load of Aβ plaques in the cerebral cortex and hippocampus than those by the FA method. In the entorhinal cortex adjacent to the subiculum, large and irregular contours of Aβ staining appeared, which were composed of fine- to coarse-granular or diffuse Aβ deposits following the PAF method. These were distributed from near the subpial layer into the deep cortex (Fig. 3G, H), which were reported as fleecy Aβ deposits (Thal et al. 1999). These Aβ deposits were only faintly or not appreciably stained following FA treatment (Fig. 3E, F). In the cerebral white matter, small but significant amounts of Aβ deposits in the diffuse or granular form were previously shown to occur (Wisniewski et al. 1989; Behrouz et al. 1991; Uchihara et al. 1995). The PAF method gave immunoreactive enhancement and revealed larger amounts of granular Aβ deposits in the cerebral white matter (Fig. 3I–L). The PAF method also enhanced Aβ immunoreactivity of ribbon-like infiltration in the subpial layer of the cerebral cortex and that of cerebral amyloid angiopathy in the vessels of the brain (data not shown). Thus, the PAF method dramatically enhanced the detection level of a spectrum of all morphological forms of Aβ deposits.

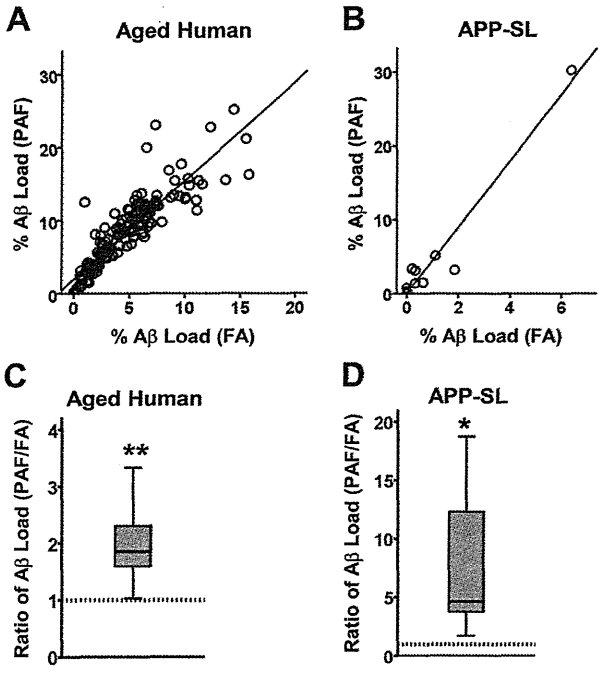

Figure 4. Effect of amyloid β peptide (Aβ) antigen retrieval (AR) by the proteinase K digestion (P), EDTA autoclaving (A), and formic acid (FA) treatment (F) (in that order; referred to as "PAF") method over that by the FA method. (A, B) In immunohistochemistry (IHC) with the 4702 antibody, Aβ loads (%) measured in the fusiform cortex of each case from the aged human brains (A) or in the hippocampus of each from the amyloid precursor protein–Swedish/London (APP-SL) mice (B) following the PAF method were plotted against those following the FA method. Significant correlations between the two AR methods were verified both in the aged human brains (Spearman rank correlation coefficient, r_s=0.92; p=9 × 10^{-69}) and in the mouse brains (r_s=0.80; p=0.003). (C, D) The effect of Aβ AR by the PAF method was significantly higher than that by the FA method both in the aged human and in the mouse brains. In IHC with the 4702 antibody, Aβ-loaded areas measured following the PAF method compared with those following the FA method (set at 1.00; the dotted lines) were 1.59-fold at the 25th percentile, 1.86-fold at the 50th percentile, and 2.31-fold at the 75th percentile in the aged human brains (C) and 3.78-fold at the 25th percentile, 4.64-fold at the 50th percentile, and 12.32-fold at the 75th percentile in the mouse brains (D). (C) Ten (≥3.39) and (D) one (92.79) outliers are not shown. **p=2 × 10^{-28}, *p=0.01; analyzed by Wilcoxon signed-rank test. n=162 from 54 individuals where three regions per case examined (A, C), and n=11 (B, D).

IHC Analysis of the AD Mouse Model by the PAF Method

We examined the brains of the AD APP-SL mice in the same way as for the AD brains. In our previous (Shin et al. 2007) and present studies using conventional Aβ IHC coupled with the FA method, younger APP-SL mice (< ~9 months) showed no occurrence of Aβ deposition, and older mice (≥ ~9 months) exhibited deposition of Aβ plaques that increased its burden with age. Application of Aβ IHC assisted by the PAF method to those younger mice also failed to reveal Aβ deposition. Therefore, in mice showing no evidence of Aβ deposition as evaluated by the FA method, the PAF method did not create any occurrence of Aβ deposition. Thus, these two methods show no difference in their ability to demonstrate the absence of Aβ deposition. In the older mice showing evidence of Aβ deposition, the PAF method was more efficient than the FA method for AR. The enhanced immunoreactive profile was shown to enlarge the sizes and to increase the numbers and immunointensities of Aβ plaques (Figs. 1E,H and 2E–H). Notably, minute Aβ plaques appeared to have a similar morphology as those seen in the AD brains. These minute plaques occur in brain samples containing significant amounts of Aβ burden and prevail dominantly with severity of Aβ burden, as was shown in the AD brain. In 9-month-old APP-SL mice that show an initial appearance of Aβ deposition, Aβ deposits were indiscernible when evaluated by the FA method. These deposits were prominently visualized as distinct Aβ deposits by the PAF method (data not shown). Thus, the PAF method could have an advantage for the retrieval of antigens in Aβ IHC in comparison with the FA method in the AD mouse model as well as humans.

Efficiency of Aβ AR by the PAF Method

We measured the areas of Aβ deposit loads in the serial sections immunostained with the 4702 antibody following the PAF or FA method, and the total sums of the Aβ-loaded areas per the whole area analyzed were compared between the two methods. In the aged human brains, Aβ deposit loads measured in the fusiform cortex by the PAF method were significantly correlated with those by the FA method (p=9 × 10^{-69}) (Fig. 4A). We compared the ratio of the Aβ deposit area from the PAF method with the ratio from the FA method. The AR effect of the PAF method (Fig. 4C) was significantly higher than that of the FA method (1.86-fold at the median) (p=2 × 10^{-28}). In the APP-SL line 7–9 mice, Aβ deposit loads measured in the whole hippocampus by the PAF method were also significantly correlated with those by the FA method (p=0.003) (Fig. 4B). The enhancing effect of the PAF method compared with that of the FA method (the ratio as described above in aged human brains) was significantly higher and 4.64-fold at the median (p=0.01) (Fig. 4D). Thus, the PAF method produced Aβ deposit loads that were consistently and significantly larger than those produced by the FA method.

Evaluation of PK versus Trypsin in Enzymatic Digestion and Some Other Solutions in Autoclave Heating

To obtain a more effective enzymatic digestion than PK digestion, we additionally tested trypsin in the double combination of enzymatic digestion and the FA method. Trypsin

digestion, when applied prior to the FA method, produced Aβ immunostaining slightly higher in its intensity than the FA method only. However, its efficacy was comparable to that of PK digestion (Suppl. Fig. S4). To obtain a more effective autoclave heating than that in the solution of 10 mM EDTA (pH 6.0) at 121C, we additionally tested solutions of EDTA (pH 3.0 and pH 10.0), DW (pH 3.0, pH 7.1, and pH 10.0), citraconic anhydride (pH 3.0, pH 7.4, and pH 10.0), and sodium citrate (pH 3.0, pH 7.2, and pH 10.0) as well as temperatures of 90C, 105C, and 121C. Among these different conditions, DW (pH 10.0 and 105C) and sodium citrate (pH 7.2 and 105C) produced high Aβ AR effects. A similar effect was observed for EDTA (pH 6.0 and 121C), although sodium citrate slightly damaged the tissue sections (Suppl. Fig. S5). The triple combinations using additional PK or trypsin digestion as the initial step produced higher Aβ AR effects than each of those double combinations, although heating in sodium citrate solution or basic water damaged the tissue sections. Further nonspecific staining was observed in the brain sections of the APP-SL mice applied by the triple combination of trypsin digestion, EDTA autoclaving, and the FA method (Suppl. Figs. S6 and S7). Thus, the triple combination of 1) PK digestion, 2) autoclave heating in 10 mM EDTA (pH 6.0 and 121C), and 3) FA treatment produced the highest Aβ AR effects without damaging tissue sections or producing nonspecific staining.

Discussion

The masking of antigens by aldehyde fixatives or by paraffin-embedding procedures is a problem for IHC studies. To overcome this problem, enzymatic digestion, FA treatment, and high-temperature heating have been developed. Among these, FA treatment is the standard method mainly used for Aβ IHC of FFPE brain tissue sections, although it was originally developed for the immunoreactive enhancement of cerebral amyloids (prion protein and Aβ) and systemic amyloids (amyloid A and prealbumin) (Kitamoto et al. 1987). The pretreatment of protein digestion with an enzyme such as trypsin had been used for IHC but only in a limited application (Battifora and Kopinski 1986; Huang et al. 1976; Mepham et al. 1979). In 1991, the advent of the heating AR method was a breakthrough in the field of IHC. Shin et al. (1991) reported that the procedure of hydrated autoclaving uncovers the masked epitopes of the microtubule-associated protein tau, showing that high-temperature heating serves as an efficient AR method. Shi et al. (1991) reported that microwave heating also shows an AR effect by testing a variety of antigens and antibodies, establishing the milestone of AR for FFPE tissue sections. Moreover, Shi et al. (1996) devised the test battery approach, which can efficiently determine the optimum protocols of AR for each antigen by comparing the immunostaining results between different kinds of solutions, temperatures, and pH (O'Leary 2001). As one good example using the test battery approach, it was demonstrated that AR procedures can also be applied to immunoelectron microscopy for amyloid deposits composed of the κ light chain or transthyretin (Rocken and Roessner 1999).

Aβ AR by FA is proposed because of the unfolding of the conformational amyloid polymers and thereby the exposing of Aβ antigens through acidic hydrolysis (Kitamoto et al. 1987). Further, FA is suggested to esterify serine residues in Aβ peptides and to alter the conformation of the amyloid polymers, as nuclear magnetic resonance imaging has revealed (Klunk et al. 1994). On the other hand, the possible mechanisms underlying AR by high-temperature heating are summarized as follows: 1) breaking of aldehyde-induced cross-linkage involving antigenic proteins, 2) extraction of diffusible blocking proteins, 3) precipitation of antigenic proteins, and 4) increased penetration of antibodies with better access to epitopes due to rehydration of the tissue sections (Suurmeijer and Boon 1993). In addition, the application of divalent/trivalent chelators in high-temperature heating removes metal ions that mask antigenic proteins (Murayama et al. 1999; Yamamoto et al. 2002; Shin et al. 2003). If autoclave high-temperature heating with EDTA chelators (Murayama et al. 1999) is then used prior to FA treatment, with the aim of affecting its activity of Aβ AR, it is likely that FA gains permeability through the tissue sections up to the unmasked Aβ fibrils. Similarly, if digestion with PK is applied prior to FA treatment, then proteolytic digestion of blocking proteins that surround Aβ fibrils might occur and unmask and thereby expose them to FA. In short, the procedures of EDTA autoclaving and PK digestion might assist the access of FA to Aβ fibrils, resulting in reinforcement of Aβ AR of FA. Indeed, we demonstrated that the combination of preceding EDTA autoclaving or PK digestion with subsequent FA treatment enhanced the AR effects of FA, and the aforementioned hypotheses might indeed be true. In support of this hypothesis, FA treatment prior to PK digestion or EDTA autoclaving gave no or only a minimally discernible enhancement in Aβ immunoreactivity compared with single FA treatment (data not shown). Our present results, together with other previous studies, show that PK digestion and EDTA autoclaving apparently differ in the mechanisms of the reinforcement of Aβ AR. If both PK digestion and EDTA autoclaving are combined with the FA method, their effects on Aβ AR by FA might be complementary rather than equivalent. Indeed, the triple combination of PK digestion and EDTA autoclaving with FA treatment provided a further stronger enhancement of Aβ AR.

Our results based on the PAF method suggest that previous IHC studies performed by the conventional FA method might have underestimated the quantitative burden of Aβ pathology and that brains with AD and its mouse models produce much more Aβ accumulation than previously assumed. Further, the presence of minute plaques revealed

by the PAF method remains to be clarified for its implication for Aβ pathology of AD and its mouse models. Notably, the molecular layer of the hippocampal dentate gyrus is the brain region that produces larger amounts of the minute plaques in the APP-SL mice than in the aged humans. This observation might explain partly, albeit not totally, why the retrieving effects differ between the human and mouse brains.

This powerful PAF method could reveal numerous SPs and various Aβ deposits that have not been detected so far. Therefore, the PAF method could serve as a sensitive IHC tool to give new insights into Aβ pathology of AD and its mouse models. We speculate that the PAF method may be the Aβ AR method with the highest efficiency so far and could be used in place of the conventional FA method.

Acknowledgments

We thank H. Kudo and H. Murayama for technical assistance and Daniel Berrar (Tokyo Institute of Technology) for the proofreading of this article and helpful comments.

Declaration of Conflicting Interests

The authors declared no potential conflicts of interest with respect to the research, authorship, and/or publication of this article.

Funding

The authors received the following financial support for the research, authorship, and/or publication of this article: This work was partially supported by the Starter Research Subvention of Tohoku University Graduate School of Medicine and Grant-in-Aid for Scientific Research on Innovative Areas (Comprehensive Brain Science Network) from the Ministry of Education, Science, Sports and Culture of Japan.

References

Ballatore C, Lee VM, Trojanowski JQ. 2007. Tau-mediated neurodegeneration in Alzheimer's disease and related disorders. Nat Rev Neurosci. 8:663–672.

Bataille F, Troppmann S, Klebl F, Rogler G, Stoelcker B, Hofstadter F, Bosserhoff AK, Rummele P. 2006. Multiparameter immunofluorescence on paraffin-embedded tissue sections. Appl Immunohistochem Mol Morphol. 14:225–228.

Battifora H, Kopinski M. 1986. The influence of protease digestion and duration of fixation on the immunostaining of keratins: a comparison of formalin and ethanol fixation. J Histochem Cytochem. 34:1095–1100.

Behrouz N, Defossez A, Delacourte A, Mazzuca M. 1991. The immunohistochemical evidence of amyloid diffuse deposits as a pathological hallmark in Alzheimer's disease. J Gerontol. 46:B209–B212.

Hardy J, Selkoe DJ. 2002. The amyloid hypothesis of Alzheimer's disease: progress and problems on the road to therapeutics. Science. 297:353–356.

Hardy JA, Higgins GA. 1992. Alzheimer's disease: the amyloid cascade hypothesis. Science. 256:184–185.

Huang SN, Minassian H, More JD. 1976. Application of immunofluorescent staining on paraffin sections improved by trypsin digestion. Lab Invest. 35:383–390.

Iwatsubo T, Odaka A, Suzuki N, Mizusawa H, Nukina N, Ihara Y. 1994. Visualization of A beta 42(43) and A beta 40 in senile plaques with end-specific A beta monoclonals: evidence that an initially deposited species is A beta 42(43). Neuron. 13:45–53.

Kang J, Lemaire HG, Unterbeck A, Salbaum JM, Masters CL, Grzeschik KH, Multhaup G, Beyreuther K, Muller-Hill B. 1987. The precursor of Alzheimer's disease amyloid A4 protein resembles a cell-surface receptor. Nature. 325:733–736.

Kitamoto T, Ogomori K, Tateishi J, Prusiner SB. 1987. Formic acid pretreatment enhances immunostaining of cerebral and systemic amyloids. Lab Invest. 57:230–236.

Klunk WE, Xu CJ, Pettegrew JW. 1994. NMR identification of the formic acid-modified residue in Alzheimer's amyloid protein. J Neurochem. 62:349–354.

Lee VM, Balin BJ, Otvos L Jr., Trojanowski JQ. 1991. A68: a major subunit of paired helical filaments and derivatized forms of normal Tau. Science. 251:675–678.

Masters CL, Simms G, Weinman NA, Multhaup G, McDonald BL, Beyreuther K. 1985. Amyloid plaque core protein in Alzheimer disease and Down syndrome. Proc Natl Acad Sci U S A. 82:4245–4249.

Mepham BL, Frater W, Mitchell BS. 1979. The use of proteolytic enzymes to improve immunoglobulin staining by the PAP technique. Histochem J. 11:345–357.

Murayama H, Shin RW, Higuchi J, Shibuya S, Muramoto T, Kitamoto T. 1999. Interaction of aluminum with PHFtau in Alzheimer's disease neurofibrillary degeneration evidenced by desferrioxamine-assisted chelating autoclave method. Am J Pathol. 155:877–885.

Namimatsu S, Ghazizadeh M, Sugisaki Y. 2005. Reversing the effects of formalin fixation with citraconic anhydride and heat: a universal antigen retrieval method. J Histochem Cytochem. 53:3–11.

O'Leary TJ. 2001. Standardization in immunohistochemistry. Appl Immunohistochem Mol Morphol. 9:3–8.

Rocken C, Roessner A. 1999. An evaluation of antigen retrieval procedures for immunoelectron microscopic classification of amyloid deposits. J Histochem Cytochem. 47:1385–1394.

Selkoe DJ. 1991. The molecular pathology of Alzheimer's disease. Neuron. 6:487–498.

Shi SR, Cote RJ, Yang C, Chen C, Xu HJ, Benedict WF, Taylor CR. 1996. Development of an optimal protocol for antigen retrieval: a 'test battery' approach exemplified with reference to the staining of retinoblastoma protein (pRB) in formalin-fixed paraffin sections. J Pathol. 179:347–352.

Shi SR, Key ME, Kalra KL. 1991. Antigen retrieval in formalin-fixed, paraffin-embedded tissues: an enhancement method for immunohistochemical staining based on microwave oven heating of tissue sections. J Histochem Cytochem. 39:741–748.